© 2014. Published by The Company of Biologists Ltd | Development (2014) 141, 685-696 doi:10.1242/dev.100297

RESEARCH ARTICLE

Cdc42/N-WASP signaling links actin dynamics to pancreatic β cell delamination and differentiation

Gokul Kesavan[1,*,], Oliver Lieven[1,2,**], Anant Mamidi[1,2], Zarah Löf Öhlin[1,2], Jenny Kristina Johansson[1], Wan-Chun Li[1,‡,§], Silvia Lommel[3], Thomas Uwe Greiner[1,¶] and Henrik Semb[1,2,‡‡]**

ABSTRACT

Delamination plays a pivotal role during normal development and cancer. Previous work has demonstrated that delamination and epithelial cell movement within the plane of an epithelium are associated with a change in cellular phenotype. However, how this positional change is linked to differentiation remains unknown. Using the developing mouse pancreas as a model system, we show that β cell delamination and differentiation are two independent events, which are controlled by Cdc42/N-WASP signaling. Specifically, we show that expression of constitutively active Cdc42 in β cells inhibits β cell delamination and differentiation. These processes are normally associated with junctional actin and cell-cell junction disassembly and the expression of fate-determining transcription factors, such as Isl1 and MafA. Mechanistically, we demonstrate that genetic ablation of N-WASP in β cells expressing constitutively active Cdc42 partially restores both delamination and β cell differentiation. These findings elucidate how junctional actin dynamics via Cdc42/N-WASP signaling cell-autonomously control not only epithelial delamination but also cell differentiation during mammalian organogenesis.

KEY WORDS: Beta cell delamination, Differentiation, Cdc42

INTRODUCTION

Delamination of individual epithelial cells from an epithelium can be the result of various morphogenetic processes such as epithelial-to-mesenchyme transition (EMT) or asymmetric cell division (Theveneau and Mayor, 2012; Wodarz and Huttner, 2003). Alternatively, delamination can be due to a cell-crowding event, in which groups of cells lose their apical surface and consequently get squeezed out of the epithelium (Marinari et al., 2012). Common to these morphogenetic processes is the requirement of active cytoskeletal rearrangements leading to dynamic changes in cell polarity, cell-cell adhesion and cell-extracellular matrix adhesion. Numerous studies have demonstrated that the Rho GTPase Cdc42 controls actin dynamics by regulating actin polymerization stability via its downstream target neuronal Wiskott-Aldrich syndrome protein (N-WASP; Wasl – Mouse Genome Informatics) *in vitro* (Kovacs et al., 2011; Rajput et al., 2013; Rohatgi et al., 1999). In *Drosophila*, Cdc42 coordinates epithelial cell rearrangement during neuroblast and notum development by stabilizing and remodeling adherens junctions (Georgiou et al., 2008; Harris and Tepass, 2008). However, how relevant Cdc42 and its target, N-WASP, are in regulating actin dynamics during epithelial cell delamination and organogenesis in mammals has not been elucidated.

Exiting of epithelial cells from an epithelium is a reiterated theme during the construction of many organs, including the pancreas. The pancreas is a glandular organ comprising both exocrine (duct and acinar cells) and endocrine (islets of Langerhans) compartments. During pancreas development, multipotent progenitor cells undergo dynamic changes in cell polarity resulting in tubulogenesis while simultaneously giving rise to both exocrine and endocrine lineages (Pan and Wright, 2011; Kesavan et al., 2009; Villasenor et al., 2010). All endocrine cells originate from neurogenin3 (Ngn3; Neurog3 – Mouse Genome Informatics)-expressing endocrine progenitors (Gradwohl et al., 2000; Gu et al., 2002). Insulin-producing β cells (Ins^+), which emerge at embryonic day (E) 13 in the mouse, exit from the pancreatic epithelium (delamination), migrate into the surrounding mesenchyme and cluster with other endocrine cells thereby forming the islets of Langerhans (Pan and Wright, 2011; Seymour and Sander, 2011; Pictet et al., 1972). Previous work has demonstrated that suppression of E-cadherin (Ecad; cadherin 1 – Mouse Genome Informatics) expression in $Ngn3^+$ cells induces basal movement within the epithelium by a process reminiscent of EMT (Gouzi et al., 2011). Furthermore, Groucho related gene 3 (Grg3; Tle3 – Mouse Genome Informatics) has been shown to act downstream of Ngn3 in suppressing Ecad expression in endocrine cells (Metzger et al., 2012). Thus, remaining questions include the identification of the signaling pathway that controls β cell delamination and its mode of action. Based on the wealth of information on the role of Cdc42/N-WASP in actin dynamics (Kovacs et al., 2011; Rohatgi et al., 1999), apical polarity (Joberty et al., 2000; Kesavan et al., 2009; Lin et al., 2000) and that apical polarity is necessary for retaining multipotent pancreatic progenitor cells within the epithelium (Kesavan et al., 2009), we hypothesized that Cdc42 inactivation drives β cell delamination.

Here, we show that preventing the hypothesized physiological inactivation of Cdc42 by expressing constitutively active (ca) Cdc42 in β cells impairs delamination of newly born β cells. Expression of caCdc42 also led to failure to disassemble junctional actin and cell-cell adhesion with diminished β cell movement. Unexpectedly, we also discovered that expression of caCdc42 cell-autonomously compromises β cell differentiation and function, resulting in hyperglycemia. The effect on β cell differentiation/function is independent of delamination as both the intra- and extra-epithelial β

[1]Stem Cell Center, Department of Laboratory Medicine, Lund University, BMC B10 Klinikgatan 26, SE-22184 Lund, Sweden. [2]The Danish Stem Cell Center, University of Copenhagen, Blegdamsvej 3B, Building 6, 4th floor, DK-2200 Copenhagen N, Denmark. [3]Institute for Cell Biology, University of Bonn, Ulrich-Haberland-Strasse 61a, 53121 Bonn, Germany.
*Present address: DFG-Center for Regenerative Therapies Dresden, Cluster of Excellence (CRTD), Biotechnology Center, Technische Universität Dresden, Fetscherstrasse 105, 01307, Dresden, Germany. ‡Present address: School of Dentistry, National Yang-Ming University, No.155, Sec. 2, Linong Street, Taipei City, 112 Taiwan, ROC. §Present address: Department of Education and Research, Taipei City Hospital, No.145, Zhengzhou Road, Datong District, Taipei City, 103 Taiwan, ROC. ¶Present address: Department of Molecular and Clinical Medicine Wallenberg Laboratory, Gothenburg University, Bruna straket 16 3tr, 413 45, Gothenburg, Sweden.
**These authors contributed equally to this work

‡‡Author for correspondence (semb@sund.ku.dk)

Received 20 June 2013; Accepted 14 November 2013

Development (2014) doi:10.1242/dev.100297

cells are impaired. Finally, we demonstrate that β cell-specific ablation of N-WASP in the caCdc42 mice rescues both delamination and β cell differentiation and function, underpinning the role of N-WASP and junctional actin in these processes *in vivo*.

RESULTS

Newborn β cells delaminate from the pancreatic epithelium to form islets

During the secondary transition stage (E13.5-15.5), the pancreatic epithelium is maturing into a naive multilayered epithelium consisting of apically polarized epithelial cells facing the lumen and epithelial cells lacking apical polarity beneath this luminal layer (Gouzi et al., 2011). We confirm that Ngn3^{+} cells, which originate from multipotent progenitors within the epithelium, exhibit both polarized and unpolarized phenotypes (Gouzi et al., 2011) (Fig. 1B). Consistent with previous work (Gouzi et al., 2011), no Ngn3^{+} cells were found outside of the epithelium (data not shown). Thus, based on the distribution of apical (Muc1) and junctional (Ecad, ZO-1, F-actin) markers, Ngn3^{+} cells displayed epithelial characteristics similar to the neighboring 'trunk cells' of the pancreatic epithelium (Fig. 1A-C). By contrast, Ins^{+} cells are unpolarized and show reduced expression of junctional markers (Ecad, ZO-1, F-actin) (Fig. 4A; supplementary material Fig. S2A). Furthermore, the majority of the Ins^{+} cells are found in clusters outside the epithelium (Fig. 1D), which later mature into islets (Fig. 1E). These observations led us to hypothesize that delamination of newly born β cells is driven by loss of apical polarity and disassembly of cell-cell junctions. As delamination and β cell differentiation and maturation occur simultaneously, we also explored whether these processes are interlinked.

Expression of caCdc42 impairs delamination of newly formed β cells

Previous work has demonstrated that Cdc42 is required for cell polarity both *in vitro* and *in vivo* (Joberty et al., 2000; Kesavan et al., 2009; Lin et al., 2000). We recently used a tamoxifen (TM)-inducible model (*Pdx1*^{CreER}; *R26R*^{lacZ}) to ablate Cdc42 in a mosaic manner within the pancreatic epithelium without perturbing the overall epithelial architecture to demonstrate that Cdc42 is required for maintaining apical polarity in pancreatic epithelial cells (Kesavan et al., 2009). Cdc42 removal also triggered delamination (Kesavan et al., 2009), suggesting that inactivation of factors crucial for apical polarity, such as Cdc42, might drive delamination. To provide experimental support for this idea, we quantified the frequency of delamination upon mosaic Cdc42 ablation and found that the majority of *Cdc42*$^{-/-}$ cells delaminate (71.33% in Cdc42$^{-/-}$/βgal^{+} versus 42% in Cdc42$^{+/-}$/βgal^{+}; supplementary material Fig. S1A,B). To test the hypothesis that β cell delamination requires inactivation of Cdc42, we expressed caCdc42 in β cells by generating transgenic (Tg) mice expressing c-Myc-tagged caCdc42 under the control of the rat insulin promoter (*RIP*^{caCdc42}; Fig. 2A). Two transgenic lines (TgA and TgB) were characterized and used throughout this study. In TgA, quantification of Ins^{+} cells co-expressing c-Myc showed that >90% of embryonic and adult β cells expressed the transgene (Fig. 2B), resulting in a threefold higher Cdc42 expression in caCdc42 compared with endogenous Cdc42 (Fig. 2C). By contrast, in the transgenic line TgB, caCdc42 was expressed in a mosaic manner (50-75%; Fig. 2B).

The consequence of expressing caCdc42 in newly born β cells was striking. Delamination of TgA β cells was significantly reduced compared with wild-type (Wt) embryos as β cells were more frequently retained within the epithelium at a luminal position [in contact with Muc1 or luminal DBA (Rps19 – Mouse Genome Informatics)] (Fig. 2D,E). Specifically, the number of β cells facing the lumen was almost tenfold higher in TgA (Fig. 2F). However, the impaired delamination phenotype was observed only in ~30% of the TgA Ins^{+} cells. We speculate that this observation can be explained by the fact that the delamination process offers limited time to turn on caCdc42 expression in all Ins^{+} cells before their exit from the epithelium.

To visualize the consequence of caCdc42 expression during delamination in real time, we used time-lapse imaging of GFP-labeled β cells (mouse insulin promoter-driven GFP; MIP-GFP) (Hara et al., 2003). As c-Myc and Ins are co-expressed in all GFP^{+} cells, GFP expression can be used as a reliable indicator of Ins^{+} transgenic β cells

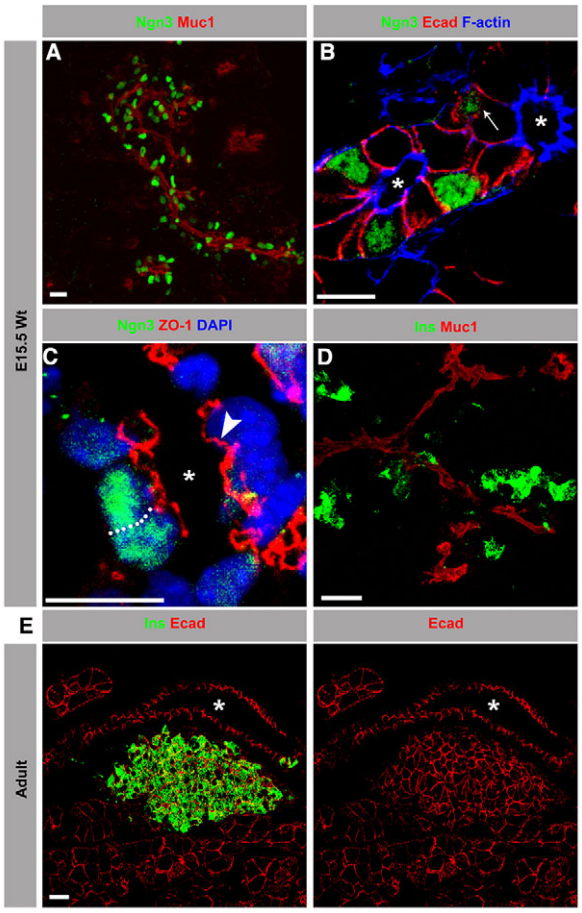

Fig. 1. Newborn β cells delaminate from the pancreatic duct epithelium to form islets. Sections from E15.5 or adult (8-week-old) wild-type (Wt) pancreas immunostained with antibodies against neurogenin 3 (Ngn3; green) or insulin (Ins; green) along with mucin 1 (Muc1; red), E-cadherin (Ecad; red), ZO-1 (red) and F-actin (blue). Images are maximum intensity projections of confocal sections acquired for the entire sample height. Asterisks indicate lumens. (A) At E15.5, Ngn3^{+} cells were exclusively found in close contact with the apical epithelial marker Muc1. (B) The majority of the Ngn3^{+} cells showed polarized distribution of apical surface F-actin and lateral Ecad, similar to neighboring 'trunk cells'. A few Ngn3^{+} cells (arrow) were distributed beneath the luminal layer, lacking the apical polarity marker F-actin. (C) The polarized distribution of ZO-1 in Ngn3^{+} cells was comparable to the fully polarized neighboring 'trunk cells' (arrowhead). The dotted line marks the cell boundary. (D) At E15.5, the majority of Ins^{+} cells resided in clusters, not associated with Muc1. Only a fraction of Ins^{+} cells were in contact with Muc1. (E) In adults, the Ins^{+} clusters matured into islets, distinctly localized from the ductal pancreatic epithelium. Scale bars: 20 μm (A,D,E); 10 μm (B,C).

Development (2014) doi:10.1242/dev.100297

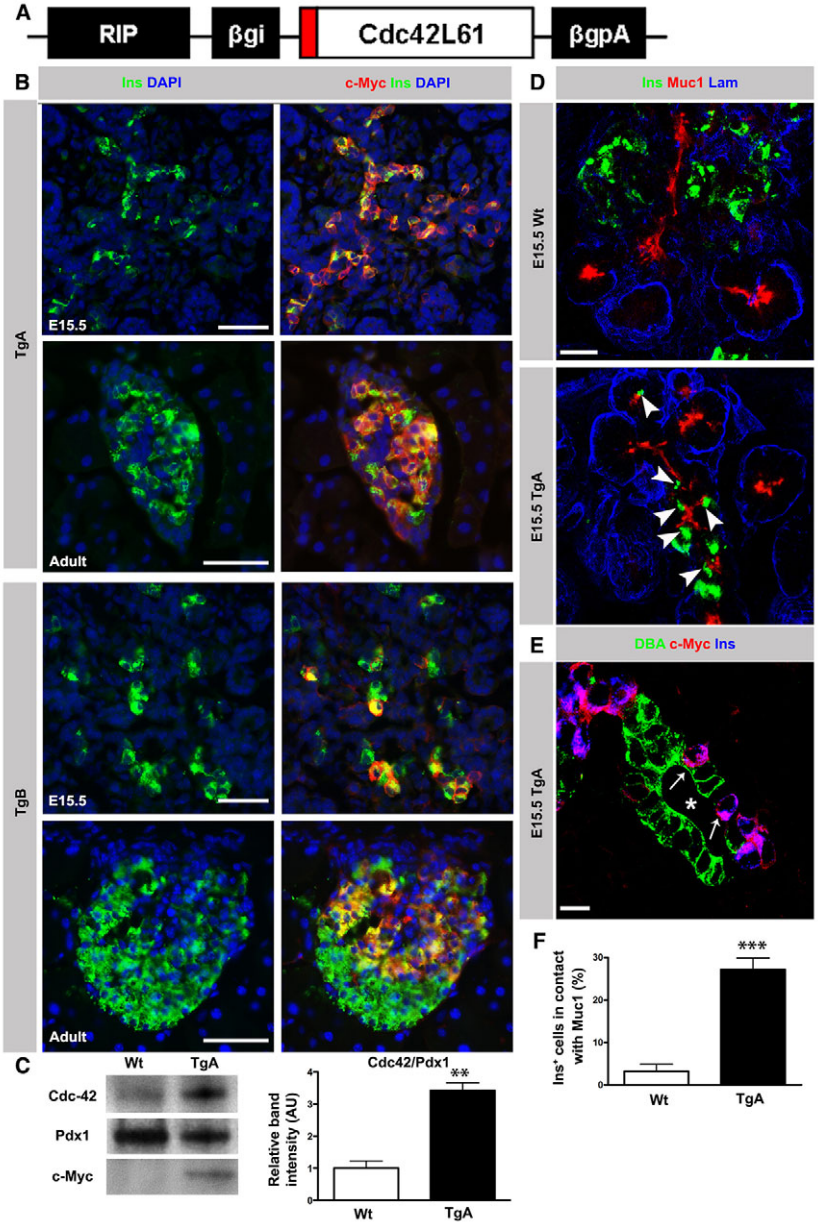

Fig. 2. Expression of constitutively active Cdc42 in pancreatic β cells impairs delamination. (A) Schematic of the transgenic construct. A c-Myc tagged (red) constitutively active form of *Cdc42* cDNA was cloned under the rat insulin promoter (RIP) along with rabbit β-globin intron (βgi) and polyA (βgpA). (B) Double immunostaining of E15.5 and adult (8-week-old) Tg pancreas sections with antibodies against c-Myc (red) and Ins (green) together with DAPI (blue). In TgA, >90% of Ins^+ cells co-expressed Ins and c-Myc. In the TgB line, co-expression of c-Myc in Ins^+ cells varied between 50 and 75%. In both Tg lines, expression of the transgene was restricted to Ins^+ cells. (C) Immunoblot analysis of Cdc42 protein expression in 8-week-old Wt and TgA islets with Cdc42, c-Myc and Pdx1 antibodies. Quantification of the Cdc42 band intensity (normalized to Pdx1) showed a threefold overexpression in TgA islets compared with Wt (n=3, $^{**}P$=0.0018). (D) Triple immunostaining of sections from E15.5 Wt and TgA pancreas with antibodies against Ins (green), Muc1 (red) and laminin (Lam; blue). In the Wt, the majority of Ins^+ cells had delaminated and cells were distributed outside the duct epithelium. A significant number of TgA Ins^+ cells remained in contact with Muc1 (arrowheads). (E) Triple immunostaining of sections from E15.5 TgA pancreas with antibodies against the duct cell marker DBA (green), c-Myc (red) and Ins (blue). TgA Ins^+ cells (arrows) were distributed between DBA^+ cells. Asterisk indicates lumen. (F) Quantification of the Ins^+ cell number facing the duct lumen (in contact with Muc-1) in serial sections of Wt and TgA E15.5 pancreas. At least 100 Ins^+ cells per pancreas of each genotype were analyzed. Data are presented as the percentage of all Ins^+ cells in contact with Muc1. About 27% of TgA Ins^+ and 3% of Wt cells were in contact with Muc1 (n=6, $^{***}P$<0.0001). Error bars represent s.e.m. Section thickness: 10 µm (B,D,E). Scale bars: 50 µm (B); 20 µm (D); 10 µm (E).

(supplementary material Fig. S1C). Real-time imaging demonstrated that Wt intra-epithelial β cells typically moved within the plane of the epithelium, often towards an extra-epithelial β cell cluster, followed by delamination and migration/clustering with other extra-epithelial β cells. By contrast, movement of TgA intra-epithelial β cells was markedly reduced, as was their ability to exit from the epithelium (Fig. 3A,B; supplementary material Movies 1, 2). Four movies from each genotype were analyzed and in each movie the number of β cells followed in real time varied from three to 25. Quantifications of the fraction of β cells that exited the epithelium revealed a 75% reduction in TgA embryos (Fig. 3C). We next used the cytoplasmic localization of GFP in the β cells to assess changes in β cell shape during migration and delamination and found that the average circularity of TgA cells was higher than that of Wt cells (0.63 in TgA versus 0.54 in Wt) (Fig. 3D). Altogether, these data suggest that expression of caCdc42 reduces β cell migration, possibly via actin dynamics (as evidenced by cell shape changes), which leads to impaired delamination.

Next, we analyzed the dynamics of cell migration during the initial stages of β cell clustering. Whereas Wt extra-epithelial β cells showed dynamic cell rearrangements (aggregation and dissociation) during the clustering process, TgA extra-epithelial cells showed minimal cell movement and less efficient aggregation into β cell clusters (supplementary material Fig. S1D). These results demonstrate that caCdc42 impairs both β cell delamination, and subsequent migration and clustering of Ins^+ cells outside the epithelium.

Impediment of cell-cell junction and cortical F-actin disassembly impairs β cell delamination *in vivo*

To understand how Cdc42 signaling may control β cell delamination, we analyzed the impact of caCdc42 expression on cell-cell junctions and actin rearrangement. At E15.5, TgA β cells showed an accumulation of cortical F-actin at cell-cell junctions independent of their position within the epithelium or in β cell clusters outside the epithelium (Fig. 4A). Quantification showed a

Development (2014) doi:10.1242/dev.100297

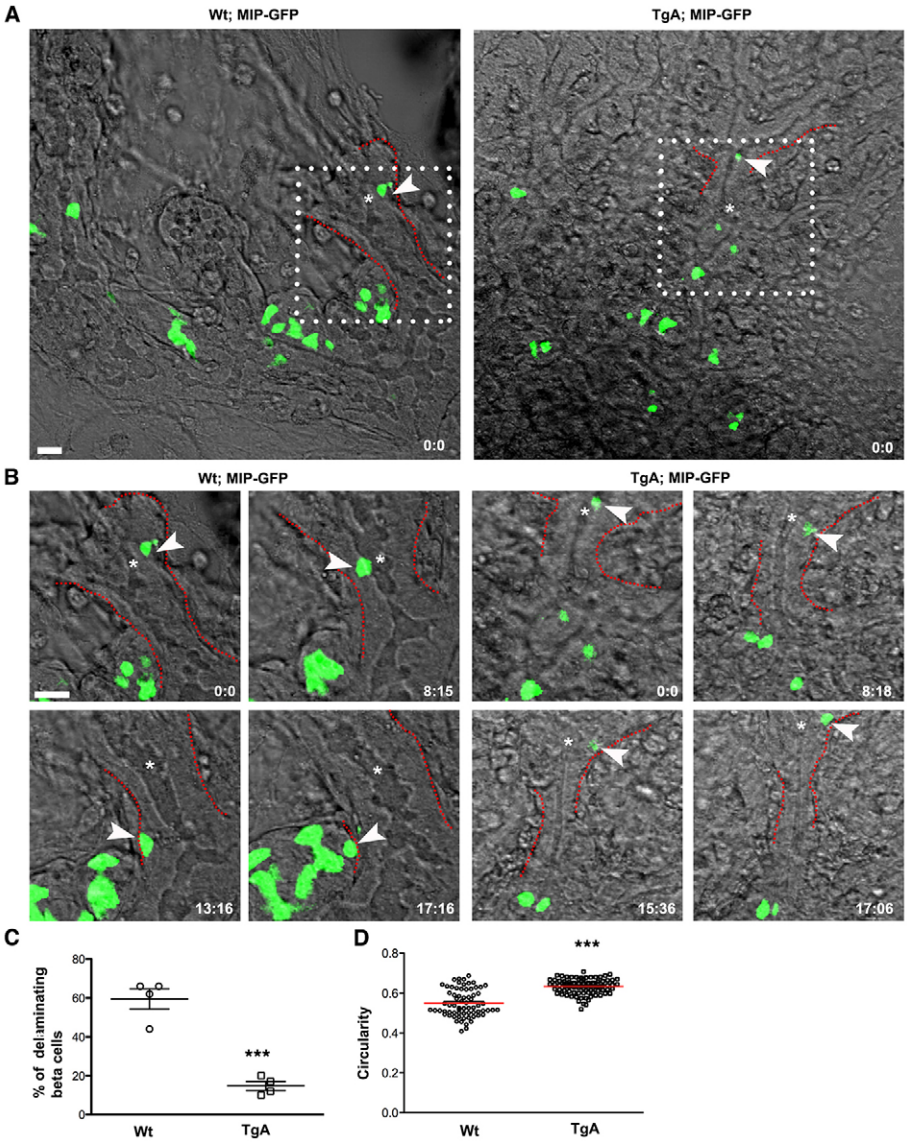

Fig. 3. Time-lapse imaging reveals impaired delamination of Ins$^+$ cells expressing caCdc42. Dorsal pancreatic explants from Wt; *MIP*^{GFP} and TgA; *MIP*^{GFP} were cultured and imaged for ~17 hours. Fluorescence and differential interference contrast images were sequentially captured every 15 minutes using *z*-stacks (35-50 µm) with an interval of 1-2 µm. The images are maximum intensity projections covering the entire sample height of 30-50 µm. (A) Snapshot at time 0, indicating the position of Ins$^+$ cells (green) relative to epithelial and mesenchymal components. White boxes indicate regions that were further analyzed using time-lapse movies (shown in B) [supplementary material Movies 1 (Wt) and 2 (TgA)]. (B) The movement of individual Wt (left) and Tg (right) Ins$^+$ cells (arrowheads) was tracked over time and representative snapshots at indicated time points (hours: minutes) are shown. Compared with Wt, TgA Ins$^+$ cell movement was markedly restricted and the cell fails to delaminate. The dotted lines (red) in A and B mark the basal boundary of the epithelium. Asterisks in A and B indicate lumen. (C) Quantification of delaminating β cells (single cells as indicated with arrowhead in A) in Wt and TgA. Delamination of β cells is significantly reduced in the TgA background (59.5% in Wt versus 14.75% in TgA; ***P=0.0002). Four movies from each genotype were analyzed. Error bars represent s.e.m. (D) Maximum intensity projections compiled from all *z*-stacks were analyzed for changes in cell shape over time using circularity as parameter; a value of one indicates a perfect circle. The average circularity of TgA cells was higher than in Wt cells. Each value in the graph represents average circularity of all Ins$^+$ cells at a given time point [*n* represents time points: Wt (70) and TgA (83), ***P<0.0001]. The red lines indicate the mean values. Scale bars: 20 µm.

twofold increase in average fluorescence intensity of F-actin in TgA β cells compared with Wt (0.12 in TgA versus 0.05 in Wt) (Fig. 4B). Transmission electron microscopy (TEM) analysis confirmed the enrichment of F-actin bundles at cell-cell junctions in TgA β cells (supplementary material Fig. S3A). By contrast, expression and distribution of Ecad and ZO-1 were unaffected in TgA β cells at E15.5 (Fig. 4B; supplementary material Fig. S2A).

Consistent with the observations at E15.5, caCdc42 expression led to an accumulation of cortical F-actin at cell-cell junctions in adult β cells (Fig. 4C; supplementary material Fig. S3B). Next, we investigated whether caCdc42 cell-autonomously or non-cell-autonomously accumulates F-actin at cell-cell junctions. For this purpose, the mosaic TgB line was used, because it provides a direct comparison between the Wt and caCdc42 cells within the same islet. In contrast to non-transgenic β cells (c-Myc$^-$Ins$^+$), increased levels of cortical F-actin and Ecad were evident in transgenic β cells (c-Myc$^+$Ins$^+$) (Fig. 4D; supplementary material Fig. S2B).

Islets of Langerhans form by endocrine cell delamination, clustering and segregation from the ducts (Greiner et al., 2009). However, in both transgenic lines, expression of caCdc42 results in intermingling of β cell clusters with ducts (supplementary material Fig. S5A,B and Fig. S4C-E), suggesting defective segregation of islet clusters from ducts. In addition, δ and α cells are randomly distributed throughout adult islets instead of their normal peripheral distribution (supplementary material Fig. S5C). Altogether, these results show that caCdc42 prevents the disassembly of the cortical actin associated with the junctional apparatus between neighboring cells, implying that dismantling of the junctional actin network is a prerequisite for β cell delamination and islet formation.

Expression of caCdc42 leads to activation of N-WASP in β cells

To unravel the underlying mechanism of how caCdc42 expression prevents the disassembly of cortical actin, we examined if caCdc42 expression led to changes in the activity and/or subcellular localization of the downstream component N-WASP. N-WASP regulates actin polymerization and is known to mediate the dynamic changes in the actin cytoskeleton associated with cell migration and cell-cell junction formation *in vitro* (Kovacs et al., 2011). In the Wt pancreas, N-WASP is localized at the apical junctional domain of large duct epithelial cells, and at lower expression levels throughout the cytoplasm in β cells (Fig. 5A). Consistently, immunoblotting

Development (2014) doi:10.1242/dev.100297

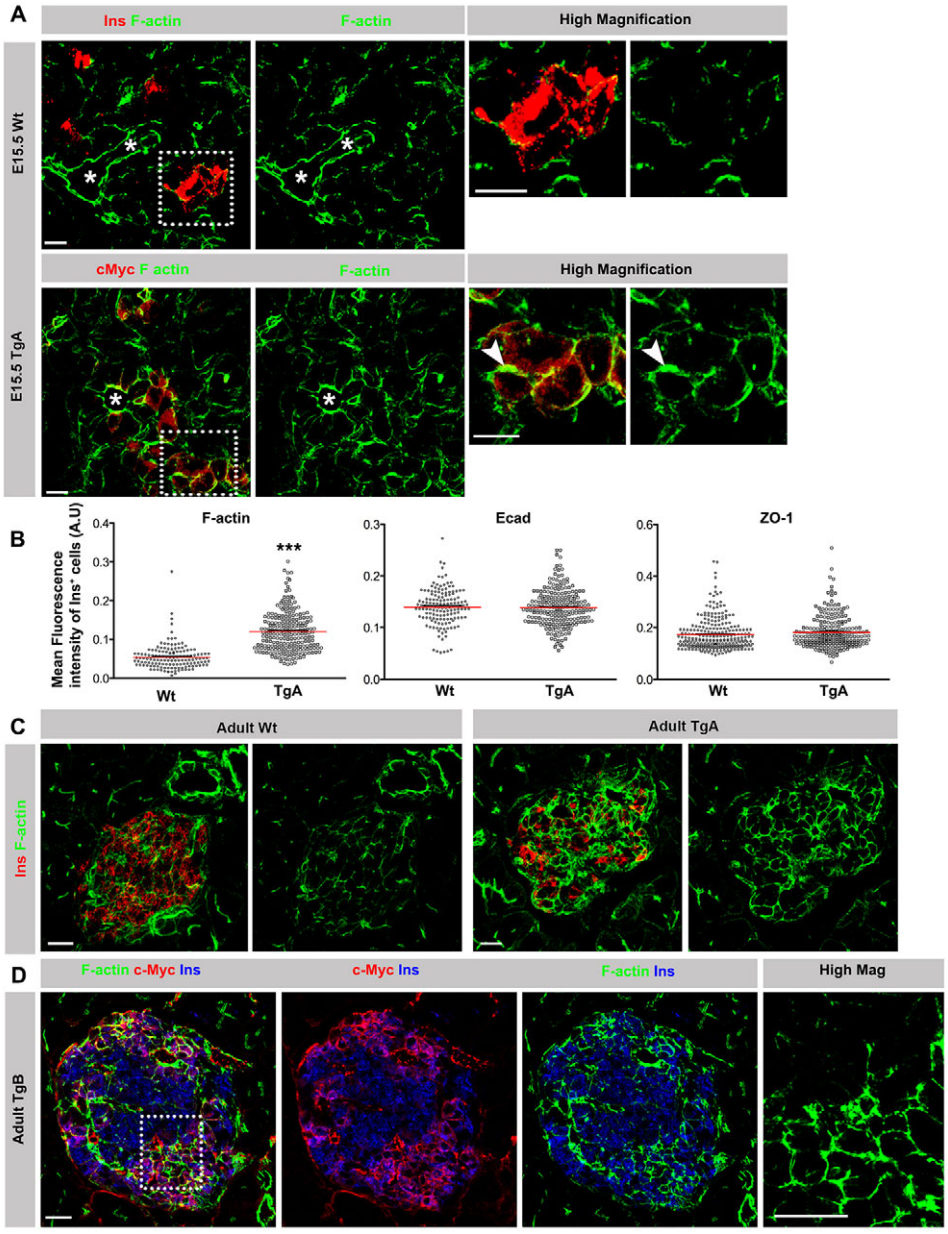

Fig. 4. Impaired cell-cell junction disassembly in caCdc42 β cells. (A) E15.5 pancreas sections from Wt and TgA immunostained with antibodies against insulin (Ins; red) or c-Myc (red) in combination with F-actin (green). In comparison to Wt β cells, TgA β cells showed enhanced cortical F-actin at cell-cell junctions (arrowheads). Asterisks indicate lumens. Dotted boxes indicate the regions shown in high magnification images. (B) Quantification of the mean fluorescence intensity of F-actin, Ecad and ZO-1 immunostainings in E15.5 Ins^+ cells revealed a significant increase of F-actin intensity in TgA Ins^+ cells compared with Wt, whereas E-cadherin and ZO-1 remained unchanged. *n* represents the number of Ins^+ cells: F-actin and Ecad, n=148 (Wt) and 217 (TgA), ***P<0.0001 (F-actin) and P=0.7345 (Ecad); ZO-1, n=264 (Wt) and 228 (TgA), P=0.1140. The red lines indicate the mean values. (C) Double immunostaining of sections from 5-week-old Wt and TgA pancreata with antibodies against F-actin (green) and Ins (red). Cortical F-actin levels were increased in all TgA Ins^+ cells compared with Wt Ins^+ cells. (D) Triple immunostaining of sections from 5-week-old TgB pancreas with antibodies against F-actin (green), c-Myc (red) and Ins (blue). TgB β cells exhibit increased levels of cortical F-actin at cell-cell contacts ($c\text{-}Myc^+Ins^+$) in comparison with Wt cells ($c\text{-}Myc^-Ins^+$). Dotted box indicates the region shown in high magnification image. Error bars represent s.e.m. The images are maximum intensity projections covering 10 µm. Scale bars: 10 µm (A,C,D).

analysis showed reduced expression of active N-WASP in endocrine cells compared with the pancreatic progenitor epithelium (Fig. 5B). By contrast, N-WASP expression/activity was significantly upregulated at cell-cell junctions in TgA β cells (Fig. 5A,B). Altogether, these results suggest that inactivation of Cdc42/N-WASP signaling is necessary for delamination of β cells *in vivo*.

Constitutively active Cdc42 interferes with β cell differentiation

To examine whether β cell delamination and differentiation are interlinked, we analyzed the differentiation status of TgA β cells ($c\text{-}Myc^+$) facing the lumen (luminal), and TgA β cells positioned outside of the epithelium (extra-epithelial) at E15.5. Notably, in a significant fraction of $c\text{-}Myc^+$ cells, insulin cannot be detected (referred to as $c\text{-}Myc^+Ins^-$ cells). Furthermore, the fraction of $c\text{-}Myc^+Ins^-$ was higher in cells facing the lumen compared with extra-epithelial cells (Fig. 6A,B). Consistently, the β cell area was significantly reduced in TgA compared with Wt embryos (Fig. 6C).

To examine if reduced insulin expression is caused by reduced expression of key β cell transcription factors, we next examined the expression of Pdx1, Nkx6.1, Isl1 and MafA at E15.5. Although expression of Pdx1 and Nkx6.1 remained unchanged, a fraction of TgA β cells show reduced expression of Isl1 compared with Wt β cells (supplementary material Fig. S4A,B; Fig. 6D). Similarly, MafA, which is only expressed in a subset of Wt Ins^+ cells at this developmental stage (Artner et al., 2010), was reduced to undetectable levels in a significant number of TgA β cells (Fig. 6D; supplementary material Fig. S4B). These results were confirmed by quantitative PCR (Q-PCR) analysis, which demonstrated reduced mRNA levels of *Ins2*, *Isl1* and *MafA*, but not *MafB*, in the E15.5 TgA pancreas (Fig. 6E). At postnatal day (P) 4, *Ins2* and *MafA* mRNA remained downregulated, whereas *Isl1* and *MafB* transcripts were comparable to Wt levels. As unchanged *Isl1* mRNA levels at P4 could be due to contribution by Isl1-expressing non-β cells, we used immunofluorescence analysis to quantify Isl1 protein expression specifically in β cells. Indeed, Isl1 protein levels were

Development (2014) doi:10.1242/dev.100297

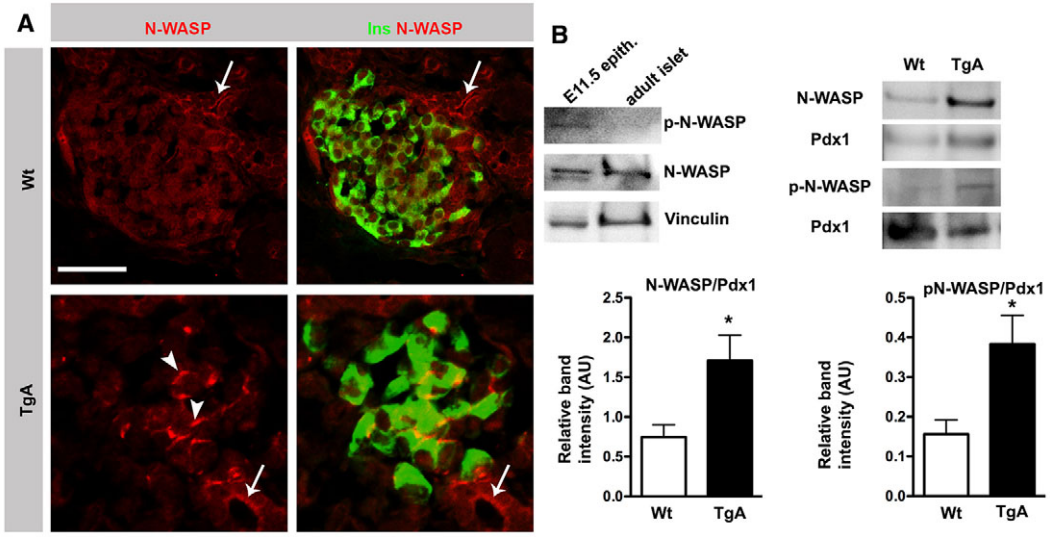

Fig. 5. Expression of caCdc42 in β cells activates N-WASP. (A) Double immunostaining of P4 Wt and TgA pancreas sections with antibodies against N-WASP (red) and insulin (Ins, green). In Wt, N-WASP is localized on the apical surface of large ducts (arrows) and the cytoplasm of β cells. In TgA, N-WASP expression in β cells is enhanced at cell-cell junctions (arrowheads). Section thickness: 10 µm. (B) Immunoblot analysis of N-WASP and phosphorylated N-WASP (p-N-WASP) protein expression in E11.5 mesenchyme-stripped pancreatic epithelia and islets, isolated from 5-week-old mice with N-WASP, p-N-WASP and vinculin antibodies (left-hand blots). In contrast to the E11.5 pancreatic epithelium, the p-N-WASP level is undetectable in isolated islets. Immunoblot analysis of islets from 8-week-old Wt and TgA mice with antibodies against N-WASP, p-N-WASP and Pdx1 showing enhanced expression of both N-WASP and p-N-WASP in TgA islets (right-hand blots). For quantification, the N-WASP and p-N-WASP band intensities were normalized to Pdx1. N-WASP, n=7, *P=0.018; p-N-WASP, n=3, *P=0.0483. Scale bar: 20 µm (A).

reduced in TgA β cells at P4 (Fig. 6F). The fact that c-Myc^{+}Ins^{-} cells are only observed during a short time-period (E15.5-16.5), suggests that these cells represent newly born β cells that rapidly turn off insulin expression leading to a 55% reduction in the number of β cells (Fig. 6C). As Isl1 and MafA are required for maturation of hormone-producing islet cells (Artner et al., 2010; Du et al., 2009), these results imply that expression of caCdc42 inhibits β cell differentiation/maturation by reducing the expression of Isl1 and MafA.

Next, we looked at the fate of the luminal TgA c-Myc^{+}Ins^{-} cells. C-Myc^{+}Ins^{-} cells do not turn on Sox9 expression (supplementary material Fig. S4C), suggesting that they do not trans-differentiate into duct cells. Cre-mediated irreversible labeling of Tg β cells with βGal (*RIP*^{Cre}; *R26R*^{lacZ}) confirmed that Tg β cells do not trans-differentiate into duct cells or other mature cell types, including acinar and non-β endocrine cells (supplementary material Fig. S4C-E; data not shown). Furthermore, caCdc42 expression had no impact on apoptosis at E15.5 (data not shown).

Constitutively active Cdc42 provokes β cell dysfunction and hyperglycemia

Analysis of postnatal β cell function showed that the number of insulin-expressing β cells is reduced and that hyperglycemia appeared at P4 (Fig. 7A,B). An increase in fasting blood glucose levels in adults as well indicates that hyperglycemia is maintained throughout life (supplementary material Fig. S5E). As hyperglycemia cannot be explained only by a 62% reduction in β cell number, the functionality of TgA islets was analyzed. TgA islets secrete less insulin under low glucose (2.8 mM glucose) conditions compared with Wt islets and fail to increase insulin secretion upon glucose-stimulation (16.7 mM glucose) (supplementary material Fig. S5F). The impaired control of insulin secretion is most likely to be caused by the reduced expression of Isl1 and MafA (Fig. 7C; supplementary material Fig. S5D), which explains the reduced number of insulin granules (Fig. 7E) as these transcription factors regulate insulin transcription, and redistribution of the glucose transporter Glut2 (Slc2a2 – Mouse Genome Informatics) from the plasma membrane to the cytoplasm (Fig. 7D).

To discriminate between direct and indirect mechanisms, we analyzed the mosaic line TgB, which does not develop hyperglycemia. In comparison to TgA β cells, a similar reduction in Isl1 and MafA expression and redistribution of Glut2 to the cytoplasm in transgenic TgB β cells was observed (Fig. 7F). These results support a cell-autonomous role for Cdc42 in β cell differentiation and function.

Ablation of N-WASP partially restores caCdc42-induced inhibition of β cell delamination and function

Based on the observation that caCdc42 expression amplifies N-WASP expression and activity in TgA β cells (Fig. 5), we speculated that increased N-WASP activity may lead to perturbed β cell delamination and differentiation via increased actin polymerization. To test this idea, we investigated whether ablation of N-WASP in β cells expressing caCdc42 rescued β cell delamination and differentiation. For this purpose, TgA mice were inter-crossed with *RIP*^{Cre}*;N-WASP*$^{fl/fl}$ mice (N-WASP βKO), referred to as TgA;N-WASP βKO. N-WASP protein was efficiently removed from most β cells in N-WASP βKO by P4 (supplementary material Fig. S6A). N-WASP removal resulted in slight changes in Isl1 expression (increase) and E-cadherin (decrease) (supplementary material Fig. S7A,B), whereas expression and distribution of F-actin, Ins, MafA and MafB remained unchanged (Fig. 8A,B; supplementary material Fig. S7B,C). However, when N-WASP is removed from TgA β cells in the 'rescue' model, TgA;N-WASP βKO, the expression and distribution of F-actin is normalized (Fig. 8A; supplementary material Fig. S6C). Next, we addressed whether delamination was

Development (2014) doi:10.1242/dev.100297

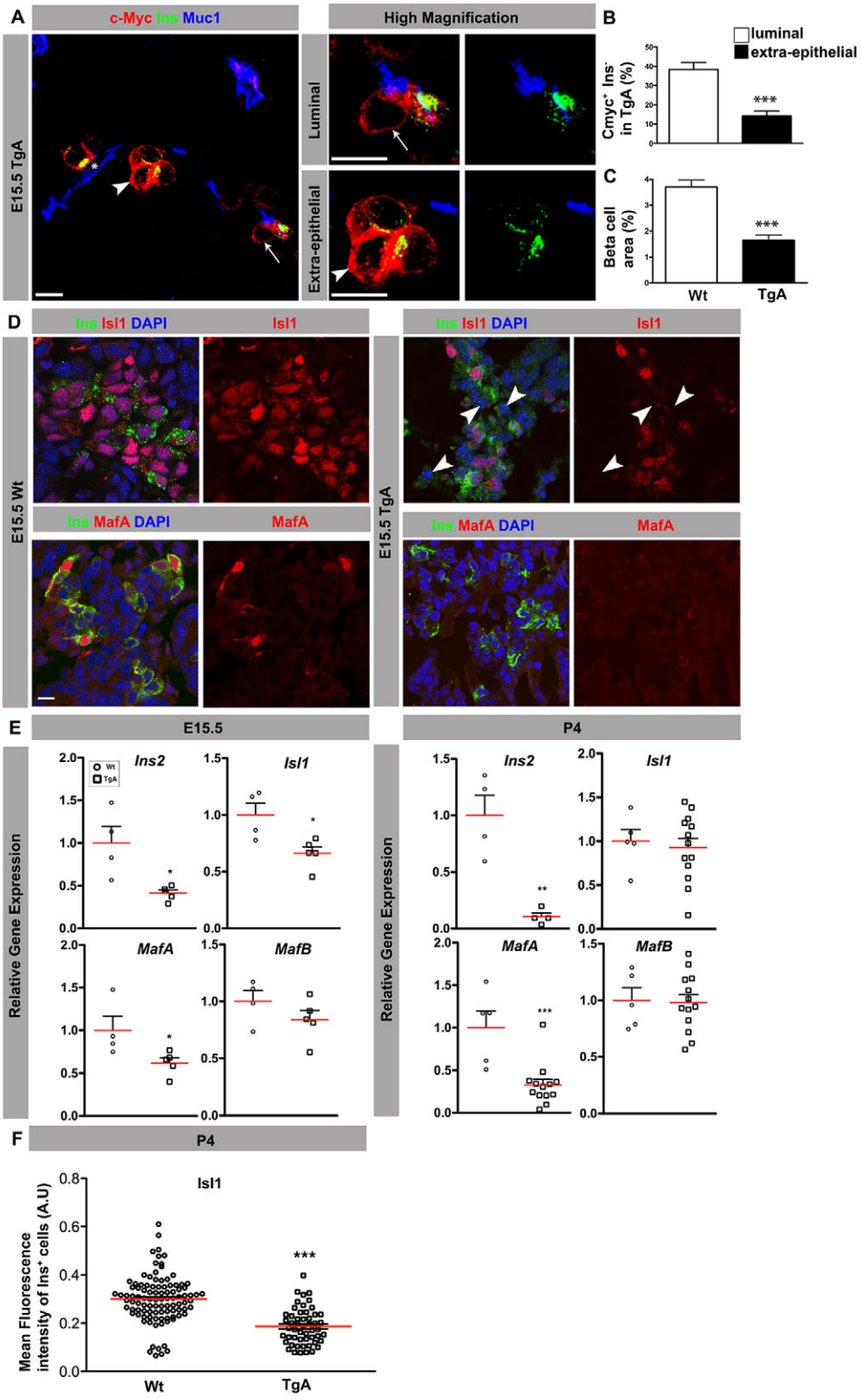

Fig. 6. Expression of caCdc42 results in deficient β cell differentiation.
(A) Triple immunostaining of sections from E15.5 TgA pancreas with antibodies against c-Myc (red), Ins (green) and Muc1 (blue). In a fraction of the c-Myc$^+$ cells, insulin is undetectable (c-Myc$^+$Ins$^-$ cells). Ins$^-$ cells were observed in both c-Myc$^+$ cells facing the lumen (luminal; arrows) and not facing the lumen (extra-epithelial; arrowheads). The indicated cells are magnified in the adjacent panels. (B) The fraction of c-Myc$^+$Ins$^-$ cells facing the lumen (luminal) and not facing the lumen (extra-epithelial) was estimated by counting the total number of c-Myc$^+$ cells and the number of luminal and extra-epithelial c-Myc$^+$Ins$^-$ cells. Loss of insulin expression was more evident in cells facing the lumen (n=5, ***P=0.0006). (C) E15.5 serial sections covering the entire pancreas were stained with Ins and Ecad antibodies. The Ins$^+$ cell area was calculated (Axiovision, Zeiss) by dividing the cross-sectional areas of β cells (Ins area) with the total pancreatic epithelium (Ecad area). The Ins$^+$ cell area is reduced in TgA mice (n=4, ***P=0.0009). (D) Sections from E15.5 Wt and TgA pancreas were immunostained with antibodies against Ins (green), Isl1 (red, upper panel), MafA (red, lower panel) and DAPI (blue). In contrast to Wt, Isl1 expression was strongly reduced in TgA Ins+ cells (arrowheads). MafA is lost in all TgA Ins$^+$ cells. (E) Q-PCR analysis of E15.5 (left) and P4 (right) Wt and TgA pancreata showed a decrease in the relative expression of *Ins2* (P=0.0128), *Isl1* (P=0.02) and *MafA* (P=0.0475), whereas *MafB* (P=0.2447) was unaffected at E15.5 (Wt, n=4; TgA, n=5). At P4, relative expressions of *Ins2* (P=0.0026) and *MafA* (P=0.0006) were decreased whereas *MafB* (P=0.8791) and *Isl1* (P=0.7083) were unaffected (Wt, n=5, for *Ins2* n=4; TgA, n=13, for *Ins2* n=4). (F) Quantification of the mean fluorescence intensity of Isl1 and Ins double immunostaining at P4 revealed a significant decrease of Isl1 expression in TgA Ins$^+$ cells compared with Wt. Three embryos for each genotype were quantified. n represents number of Ins$^+$ cells: n=100 (Wt) and n=52 (TgA), ***P<0.0001. The red lines indicate mean values. The images are maximum intensity projections covering 10 µm. Scale bars: 10 µm.

rescued in TgA;N-WASP βKO mice by quantifying the number of β cells facing the lumen. Indeed, fewer β cells face the lumen in TgA;N-WASP βKO compared with TgA mice, suggesting that removal of N-WASP in the TgA β cells ameliorates delamination (Fig. 8C; supplementary material Fig. S6B). Furthermore, to explore whether N-WASP mediates caCdc42-induced β cell dysfunction, we tested if N-WASP ablation restored expression of Glut2, Isl1 and MafA. Whereas ablation of N-WASP in β cells (N-WASP βKO) resulted in a slight increase in Isl1 expression (Fig. 8A,B,D), removal of N-WASP in TgA β cells (TgA;N-WASP βKO) partially normalized expression of Isl1, Glut2 and MafA (Fig. 8A,B,D). Consistent with these observations, blood glucose levels were also

Development (2014) doi:10.1242/dev.100297

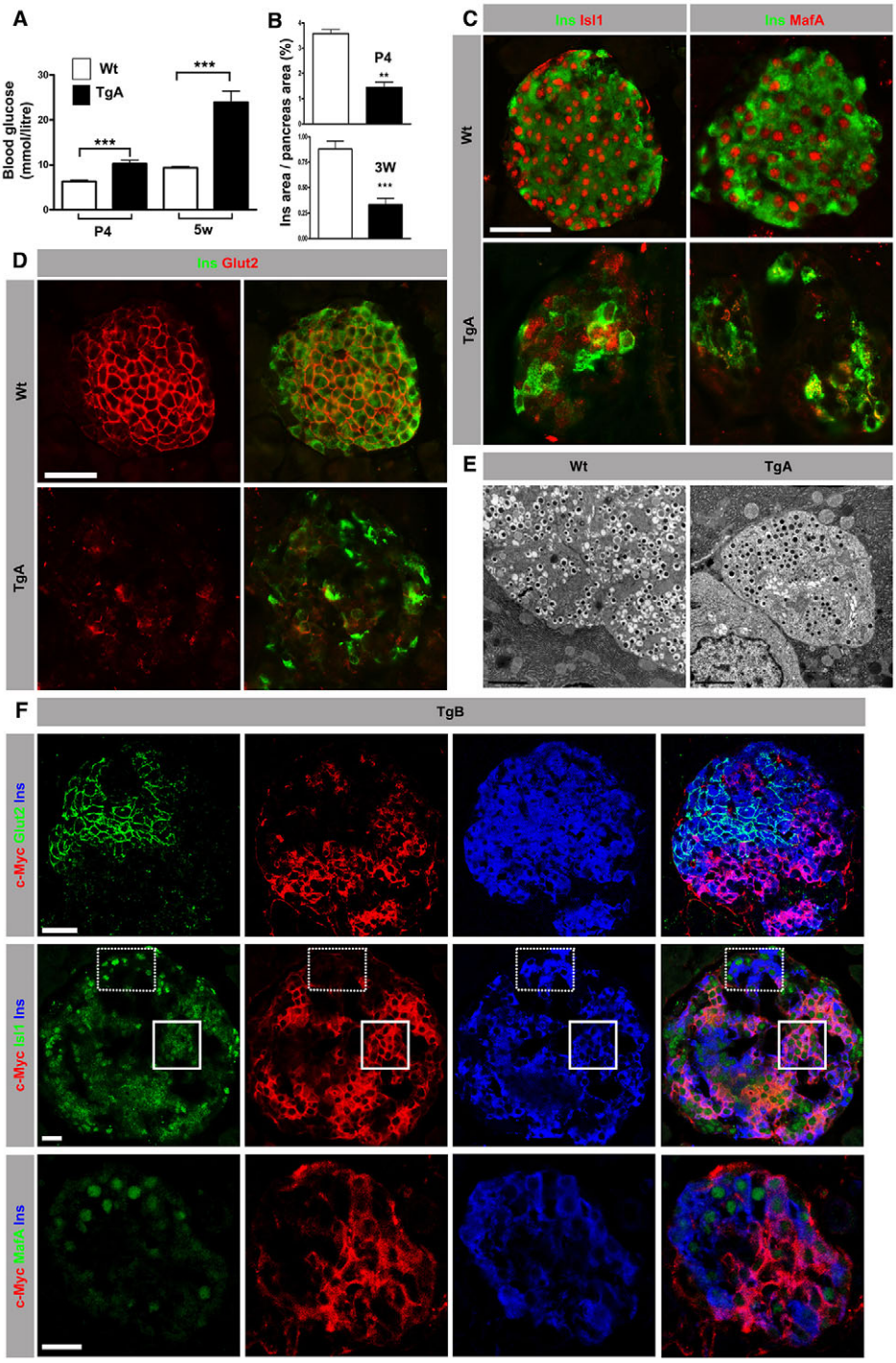

Fig. 7. Expression of caCdc42 instigates β cell dysfunction and hyperglycemia. (A) Random blood glucose measurements at P4 and at 5 weeks (5w) in Wt and TgA mice. TgA animals show elevated blood glucose levels at both time points (n=10; for P4 ***P=0.0003 and 5w ***P<0.0001). (B) The Ins$^+$ cell area was calculated from serial sections of the entire pancreas stained with Ins and Ecad antibodies. TgA animals exhibit a reduced Ins$^+$ cell area at both P4 and 3 weeks (3W) of age (P4, n=3, **P=0.0015; 3W, n=5, ***P=0.0007). (C) Double immunostaining of sections from 8-week-old mice with antibodies against Isl1 (red, left panels) or MafA (red, right panels) with Ins (green). Wt Ins$^+$ cells show nuclear localization of Isl1 and MafA, whereas Isl1 and MafA expression is significantly reduced in TgA Ins$^+$ cells. (D) Double immunostaining of sections from 8-week-old mice with antibodies against Glut2 and Ins (green). In contrast to Wt, TgA Ins$^+$ cells show diffuse cytoplasmic Glut2 expression. (E) TEM analysis of 5W islets shows reduced number of insulin granules in the TgA Ins$^+$ cells compared with Wt Ins$^+$ cells. (F) Triple immunostaining of sections from TgB pancreas of 5-week-old mice with antibodies against Glut2 (green, top panel), Isl1 (green, middle panel) or MafA (green, bottom panel) combined with c-Myc (red) and Ins (blue). c-Myc$^+$Ins$^+$ cells express reduced levels of Glut2, Isl1 and MafA compared with c-Myc$^-$Ins$^+$ cells. Solid and dotted squares represent areas with TgB (c-Myc$^+$Ins$^+$) and Wt (c-Myc$^-$Ins$^+$) cells, respectively. Images were acquired using a confocal microscope. Section thickness: 10 µm (C,D,F). Error bars show s.e.m. Scale bars: 20 µm (C,D,F); 2 µm (E).

partially normalized in TgA;N-WASP βKO mice (Fig. 8E). In summary, these results identify N-WASP as a key downstream effector of caCdc42 during β cell delamination and differentiation, and underpin the role of cortical F-actin dynamics in this process.

DISCUSSION

Based on our findings, we propose a model for β cell delamination in which activated Cdc42 (Cdc42-GTP), via N-WASP, retains multipotent progenitors within the epithelium by maintaining apical polarity and stable cortical F-actin and cell-cell junctions. Delamination of newly born β cells is initiated by the inactivation of Cdc42 (Cdc42-GDP) and the effector N-WASP, which results in loss of apical polarity, and disassembly of the cortical F-actin network and cell-cell junctions (supplementary material Fig. S7D). β cell differentiation and function also depend on Cdc42/N-WASP inactivation, but without being physically linked to the delamination process (Fig. 8F).

Previous studies have demonstrated that Cdc42 is involved in apical cell polarity and cell movement within the plane of a multi-layered neuro-epithelium, which in turn decides lineage commitment depending on the apical or basal position of the cell (Cappello et al., 2006; Harris and Tepass, 2008). However, the exact

Development (2014) doi:10.1242/dev.100297

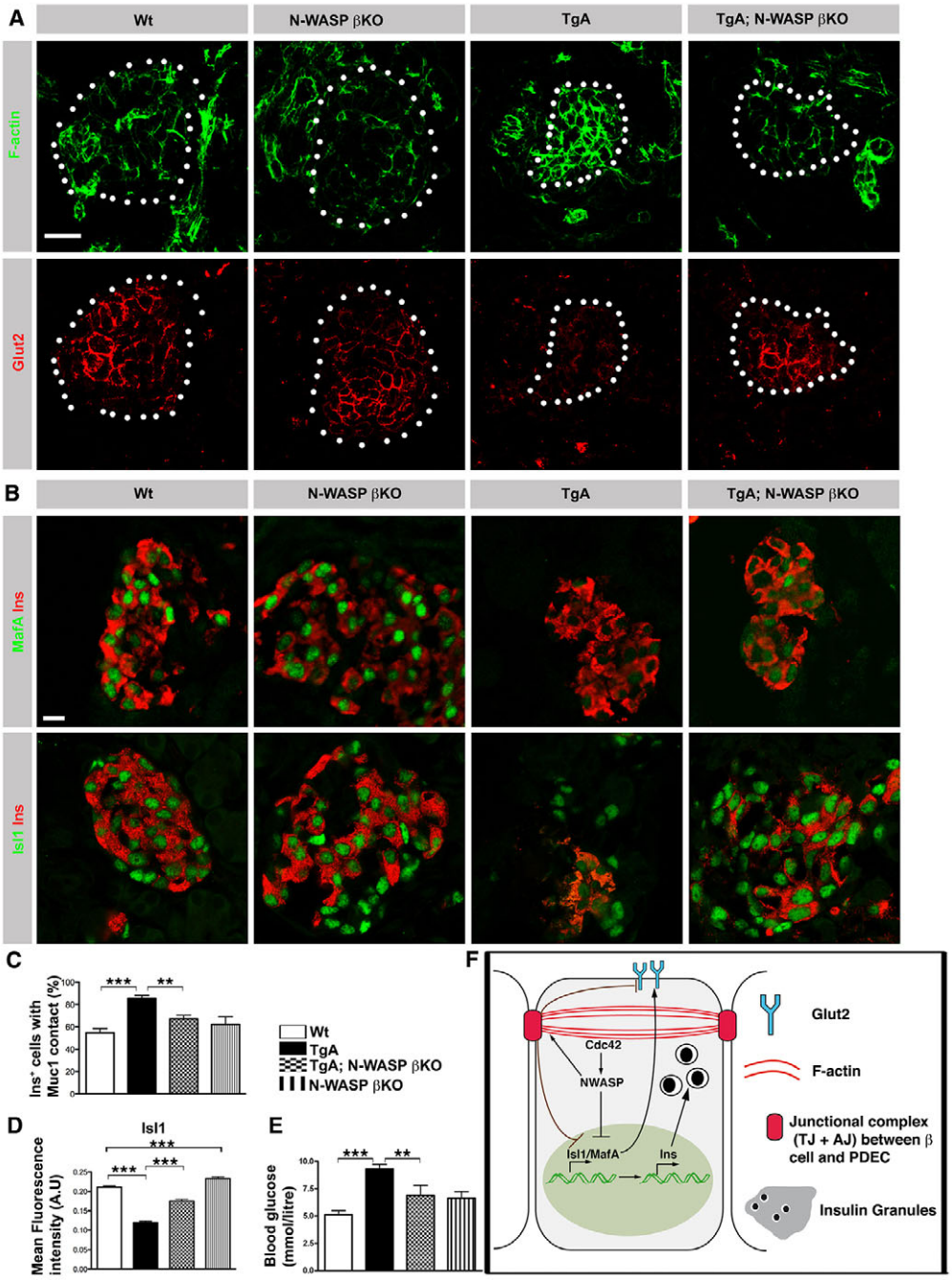

Fig. 8. Ablation of N-WASP partially restores caCdc42-induced inhibition of β cell delamination and differentiation. (A) Sections of P4 Wt, N-WASP βKO, TgA and TgA;N-WASP βKO pancreata were immunostained with antibodies against F-actin (green) and Glut2 (red). Islets are marked with dotted circles and were identified using Ins staining (supplementary material Fig. S7D). Wt and N-WASP βKO Ins$^+$ cells show similar expression levels/subcellular distributions of F-actin and Glut2. TgA Ins$^+$ cells show increased F-actin and reduced Glut2. F-actin and Glut2 expression levels/distribution of Ins$^+$ cells is partially restored in TgA;N-WASP βKO. (B) Sections from P4 Wt, N-WASP βKO, TgA and TgA;N-WASP βKO pancreata were immunostained with antibodies against MafA (green, upper panels), Isl1 (green, lower panels) and Ins (red). Isl1 expression is restored to Wt levels in TgA;N-WASP βKO Ins$^+$ cells in comparison with TgA Ins$^+$ cells, whereas MafA expression is partially restored. (C) Quantification of the Ins$^+$ cell number facing the lumen (in contact with Muc1) in serial sections of P4 Wt, TgA, TgA; N-WASP β KO and N-WASP β KO pancreata. Only individual or doublet Ins$^+$ cells were counted as the majority of the Ins$^+$ cells had delaminated and clustered into islet-like structures. The data are expressed as the percentage of all single and doublet Ins$^+$ cells (excluding Ins$^+$ in clusters) that are in contact with Muc1; 54% Wt (n=4), 85% TgA (n=7), 67% TgA;N-WASP βKO (n=8) and 62% N-WASP βKO (n=3). Wt versus TgA, ***P=0.0001, TgA versus TgA;N-WASP βKO, **P=0.0014. (D) Mean fluorescence intensity quantification of the Isl1 and Ins double immunostaining shown in B. Isl1 expression in Ins$^+$ cells was reduced in TgA compared with Wt and was restored in TgA;N-WASP βKO. n represents number of Ins$^+$ cells (pooled): at least 500 Ins$^+$ were counted for each genotype, ***P<0.0001. (E) Random blood glucose measurements at P4. The elevated blood glucose levels observed in TgA mice was partially restored in TgA;N-WASP βKO mice (Wt and TgA, n=15; N-WASP βKO, n=4; TgA;N-WASP βKO, n=5; Wt versus TgA, ***P=0.0001; TgA versus TgA;N-WASP βKO, **P=0.0150). (F) Schematic of how caCdc42 cell-autonomously affects β cell differentiation/maturation and function. Cdc42 regulates expression of key β cell transcription factors, including Isl1 and MafA, and their targets (e.g. insulin) and Glut2 via N-WASP. The images are maximum intensity projections covering 10 µm. Error bars represent s.e.m. Scale bars: 20 µm.

Development (2014) doi:10.1242/dev.100297

role of cell-autonomous and non-cell-autonomous factors in controlling lineage commitment has not been resolved. In this study, we show for the first time that Cdc42/N-WASP-mediated actin dynamics cell-autonomously control cell differentiation *in vivo*. Furthermore, the observation that β cell delamination is partly normalized by preventing N-WASP activation upon Cdc42 activation provides the first evidence that N-WASP is a major effector of Cdc42 during epithelial cell delamination *in vivo*.

We further demonstrate that the delamination process per se is uncoupled from cell differentiation *in vivo* as Isl1 and insulin expression are dramatically reduced in both intra- and extra-epithelial transgenic β cells at E15.5. Furthermore, mosaic expression of caCdc42 cell-autonomously increases the actin network at cell-cell contacts, and inhibits the expression of Isl1, MafA, Glut2 and insulin.

Based on the fact that reduced N-WASP activity correlates with a drop in the levels of junctional Ecad and F-actin during β cell birth, we speculate that the β cell-specific ablation of N-WASP removes an already reduced pool of active N-WASP, which limits significant additional impacts on F-actin, Ecad, Isl1 and MafA. The mechanism for how N-WASP controls junctional Ecad might involve direct binding of N-WASP to Ecad (Georgiou et al., 2008; Kovacs et al., 2011). Thus, the results from the β cell-specific ablation of N-WASP, although minor, together with the changes in N-WASP expression/activity during normal β cell development, suggest that N-WASP plays a physiological role in β cell birth.

The partial rescue of caCdc42-induced cortical actin and impaired β cell differentiation by ablating N-WASP in β cells can be explained by several mechanisms. First, N-WASP is only one of several components downstream of Cdc42 (e.g. several PAK family members act downstream of Cdc42) (Etienne-Manneville, 2004); therefore, other Cdc42 targets might affect β cell delamination and differentiation. Second, technical aspects, including the efficiency of Cre-mediated ablation of N-WASP in β cells (timing and fraction of β cells), may also contribute to the partial rescue.

Expression of caCdc42 in β cells results in hyperglycemia, which is caused by reduction in β cell mass and by β cell dysfunction. Our data suggest that the latter is caused by reduced insulin expression as well as Glut2 mislocalization. The facts that Isl1 binds to the MafA promoter (Du et al., 2009) and that MafA binds to the insulin promoter (Artner et al., 2008; Matsuoka et al., 2007) suggest that the reduction in insulin expression and number of insulin granules upon caCdc42 expression is indirectly caused by diminished expression of Isl1 and MafA.

Several lines of evidence suggest that forces transmitted across cell-extracellular matrix and cell-cell adhesion sites result in cellular cytoskeletal stiffness adjustments, and vice versa. Specifically, the F-actin/myosin-dependent contractile forces are mainly responsible for generating mechanical tension in cells, which then affects the expression of mechanotransduction pathways, including YAP/TAZ, MAL/SRF and NF-κB (Dupont et al., 2011). Hence, we speculate that the transcriptional machinery involved in β cell differentiation/maturation, specifically Isl1 and MafA transcription, may depend on changes in mechanical and physical influences mediated by junctional actin dynamics. Future studies should consider the impact of mechanotransduction in β cell development. It is likely that similar mechanisms for regulating cell specification will apply to other tissue and organ systems *in vivo* as well.

MATERIALS AND METHODS

Transgenic mice

To express constitutively active Cdc42 in pancreatic β cells, the *Cdc42L61* (Lamarche et al., 1996) cDNA was subcloned under the control of the rat insulin promoter (RIP) (Hanahan, 1985). A c-Myc tag fused to the N-terminal end of the Cdc42L61 was used to monitor transgene expression. Rabbit β-globin intron (βgi) and polyA (βgpA) were inserted along with the cDNA to increase expression of the transgene. Transgenic mice were generated at the Lund University transgenic core facility. Eight transgenic founder lines were identified by PCR and confirmed by Southern blot (data not shown). Two highly expressing transgenic lines were chosen for the experiments and transgene expression was confirmed by immunohistochemistry and immunoblotting. Mice were backcrossed against C57Bl/6J or DBA/2J backgrounds and wild-type littermates were used as controls.

Pdx1-cre ER^{TM}-mediated Cdc42 depletion was carried out as previously described (Kesavan et al., 2009). TgA;N-WASP βKO mice were generated by crossing *N-WASP*$^{fl/fl}$ mice (Lommel et al., 2001) with *RIP*^{Cre} mice (Herrera, 2000) to obtain β cell-specific N-WASP knockout (KO) mice, referred to here as N-WASP βKO. N-WASP βKO mice were crossed with *RIP*^{caCdc42} to generate TgA;N-WASP βKO. Animals were maintained in an approved animal facility and all animal work was carried out in accordance with the local ethics committee for animal research.

Lineage tracing

R26R^{lacZ} mice (Soriano, 1999) were crossed with *RIP*^{Cre} (Herrera, 2000) and *RIP*^{caCdc42} (both TgA or TgB) mice to obtain *RIP*^{caCdc42}; *R26R*^{lacZ}; *RIP*^{Cre} mice. The recombined cells were identified using a β-galactosidase antibody or by X-gal staining.

Blood glucose measurements

Random blood glucose was measured using a hand-held glucometer (OneTouch Ultra; Lifescan). Blood was obtained from the tail vein (5-week-old mice) or collected after the pups were sacrificed. Fasting blood glucose was measured after the mice were starved overnight.

Immunohistochemistry

Tissues were fixed, sectioned and processed as previously described (Kesavan et al., 2009). Details of antibodies used are given in supplementary material Table S1. Stained sections were imaged in an AxioplanII fluorescent microscope or LSM510 or LSM780 laser scanning microscope and the images were analyzed using Axiovision LE software (Zeiss) or Imaris (Bit-plane).

Quantification of mean fluorescence intensity

F-actin, E-cadherin and ZO-1 mean fluorescence intensity quantifications of E15.5 Wt and TgA Ins$^+$ cells was performed using cellprofiler software (Carpenter et al., 2006). Sections were immunostained simultaneously under constant conditions (at least n=3 embryos/genotype). Ins$^+$ cells were identified as the primary object and F-actin, Ecad and ZO-1 intensities were quantified. The mean differences were tested for statistical significance using Student's t-test. Similar analysis was carried out to measure the Isl1 intensity at P4.

Quantification of cell shape changes over time

Maximum intensity projections were compiled using z-stacks from real time images. ImageJ (analyze particles) was used to quantify differences in cell shape changes over time. The average circularity of all Ins$^+$ cells was calculated for all the time points and mean differences were tested for statistical significance using Student's t-test.

Morphometric analysis

To quantify Ins$^+$ cell areas in embryonic and adult pancreas, serial sections spanning the entire tissue were made and stained for insulin and E-cadherin. The cross-sectional areas from the acquired images were measured using Axiovision Software (Zeiss). To quantify apically localized insulin cells, E15.5 and P4 pancreas sections from Wt and caCdc42 embryos were stained for Muc1 and Ins, and the number of Ins$^+$ cells in direct contact with Muc1 was counted.

Transmission electron microscopy

Embryonic and adult pancreata were fixed and processed as previously described (Kesavan et al., 2009).

Explant cultures and real-time imaging

Real-time imaging of β cell delamination was performed using E11.5 dorsal pancreata from *MIP*^{GFP} (Hara et al., 2003) and TgA/*MIP*^{GFP} mice and cultured on fibronectin-coated coverslips (Percival and Slack, 1999). The day of the harvest (E11.5) was marked as day 0. Starting from day 5, the explants were imaged for ~17 hours using a Zeiss Laser Scanning Microscope (LSM 780). The imaging was carried out in a humidified, heated chamber with CO_2 using a 20× objective. *Z*-stacks of 1-2 µm thickness were acquired for the entire sample height of 35-50 µm. The images were analyzed and maximum intensity projections of all time points were exported in Quicktime format using Imaris software (Bit-plane).

Isolation of islets

Islets were isolated from transgenic and control mice using standard protocols as previously described (Greiner et al., 2009).

Glucose-mediated insulin secretion assay *in vitro*

Isolated islets (Wt: 150-280 islets per animal, n=4; TgA: 15-60 islets per animal, n=5) of comparable size and morphology were selected for the insulin secretion assay. Islets were cultured in RPMI 1640 media containing 10% fetal bovine serum, 1% Penicillin-Streptomycin and 11.1 mM glucose and incubated overnight at 37°C. The media was exchanged with assay buffer (114 mM NaCl, 4.7 mM KCl, 1.2 mM KH_2PO_4, 1.16 mM $MgSO_4$, 20 mM HEPES, 0.2% bovine serum albumin; pH 7.2), containing 3.3 mM glucose and incubated for 2 hours at 37°C. Three islets per well were transferred to flat-bottom 96-well cell plates containing assay buffer, with either 2.8 mM or 16.7 mM glucose (n=10), and incubated at 37°C for 1 hour. The culture supernatant was used for insulin ELISA measurements (Mercodia, Uppsala, Sweden). Secreted insulin concentrations were normalized to per islet and mean differences were tested for statistical significance using Student's *t*-test.

Immunoblotting

Isolated islets and E11.5 mesenchyme-stripped pancreatic epithelia were lysed in sample buffer, separated on SDS-PAGE and electro-transferred using standard protocols. The band intensities were calculated using the ImageJ software.

Quantitative PCR

RNA extraction was performed according to manufacturer's protocol (Qiagen). cDNA was prepared using Superscript II (Invitrogen) with random hexamers. Real-time PCR was performed in an ABI PRISM 7900 using SYBR Green. Primer sequences are listed in supplementary material Table S2.

Statistics

Data are presented as mean + s.e.m. All statistical analysis was performed using two-tailed, unpaired, Student's *t*-test in Graphpad Prism software. *P*-values less than 0.05 were considered significant.

Acknowledgements

We thank P. Aspenstrom for the caCdc42 construct; C. Wright and Beta Cell Biology Consortium (BCBC) for providing antibodies; R. Matsson from the Lund transgenic core facility; C. Brakebusch for Cdc42 floxed mice; R. Sczech for image analysis; I. Artner and P. Serup for comments on the manuscript; V. Iyengar for language and content editing; E. Ganic for Q-PCR, M. Magnusson, J. Esfandyari, A. Stiehm and the Lund Animal facilities and R. Wallen for TEM.

Competing interests

The authors declare no competing financial interests.

Author contributions

G.K., O.L. and H.S. conceived the project and designed experiments. G.K., O.L., A.M., Z.L.Ö., J.K.J., W.-C.L. and T.U.G. performed experiments and analyzed the data. S.L. contributed reagents for experiments with N-WASP knockout. G.K., O.L. and H.S. wrote the manuscript.

Funding

This work was supported by the Swedish Research Council; Lund University Stem Cell Center; Swedish Foundation for Strategic Research; National Institutes of Health/National Institute of Diabetes and Digestive and Kidney Diseases (NIDDK) as part of the Beta Cell Biology Consortium [DK089570]; Juvenile Diabetes Research Foundation [17-2011-627]; Novo Nordisk Foundation; and Danish Strategic Research Council.

Supplementary material

Supplementary material available online at
http://dev.biologists.org/lookup/suppl/doi:10.1242/dev.100297/-/DC1

References

Artner, I., Hang, Y., Guo, M., Gu, G. and Stein, R. (2008). MafA is a dedicated activator of the insulin gene in vivo. *J. Endocrinol.* **198**, 271-279.

Artner, I., Hang, Y., Mazur, M., Yamamoto, T., Guo, M., Lindner, J., Magnuson, M. A. and Stein, R. (2010). MafA and MafB regulate genes critical to beta-cells in a unique temporal manner. *Diabetes* **59**, 2530-2539.

Cappello, S., Attardo, A., Wu, X., Iwasato, T., Itohara, S., Wilsch-Bräuninger, M., Eilken, H. M., Rieger, M. A., Schroeder, T. T., Huttner, W. B. et al. (2006). The Rho-GTPase cdc42 regulates neural progenitor fate at the apical surface. *Nat. Neurosci.* **9**, 1099-1107.

Carpenter, A. E., Jones, T. R., Lamprecht, M. R., Clarke, C., Kang, I. H., Friman, O., Guertin, D. A., Chang, J. H., Lindquist, R. A., Moffat, J. et al. (2006). CellProfiler: image analysis software for identifying and quantifying cell phenotypes. *Genome Biol.* **7**, R100.

Du, A., Hunter, C. S., Murray, J., Noble, D., Cai, C. L., Evans, S. M., Stein, R. and May, C. L. (2009). Islet-1 is required for the maturation, proliferation, and survival of the endocrine pancreas. *Diabetes* **58**, 2059-2069.

Dupont, S., Morsut, L., Aragona, M., Enzo, E., Giulitti, S., Cordenonsi, M., Zanconato, F., Le Digabel, J., Forcato, M., Bicciato, S. et al. (2011). Role of YAP/TAZ in mechanotransduction. *Nature* **474**, 179-183.

Etienne-Manneville, S. (2004). Cdc42 - the centre of polarity. *J. Cell Sci.* **117**, 1291-1300.

Evan, G. I., Lewis, G. K., Ramsay, G. and Bishop, J. M. (1985). Isolation of monoclonal antibodies specific for human c-myc proto-oncogene product. *Mol. Cell. Biol.* **5**, 3610-3616.

Georgiou, M., Marinari, E., Burden, J. and Baum, B. (2008). Cdc42, Par6, and aPKC regulate Arp2/3-mediated endocytosis to control local adherens junction stability. *Curr. Biol.* **18**, 1631-1638.

Gouzi, M., Kim, Y. H., Katsumoto, K., Johansson, K. and Grapin-Botton, A. (2011). Neurogenin3 initiates stepwise delamination of differentiating endocrine cells during pancreas development. *Dev. Dyn.* **240**, 589-604.

Gradwohl, G., Dierich, A., LeMeur, M. and Guillemot, F. (2000). neurogenin3 is required for the development of the four endocrine cell lineages of the pancreas. *Proc. Natl. Acad. Sci. USA* **97**, 1607-1611.

Greiner, T. U., Kesavan, G., Ståhlberg, A. and Semb, H. (2009). Rac1 regulates pancreatic islet morphogenesis. *BMC Dev. Biol.* **9**, 2.

Gu, G., Dubauskaite, J. and Melton, D. A. (2002). Direct evidence for the pancreatic lineage: NGN3+ cells are islet progenitors and are distinct from duct progenitors. *Development* **129**, 2447-2457.

Hanahan, D. (1985). Heritable formation of pancreatic beta-cell tumours in transgenic mice expressing recombinant insulin/simian virus 40 oncogenes. *Nature* **315**, 115-122.

Hara, M., Wang, X., Kawamura, T., Bindokas, V. P., Dizon, R. F., Alcoser, S. Y., Magnuson, M. A. and Bell, G. I. (2003). Transgenic mice with green fluorescent protein-labeled pancreatic beta -cells. *Am. J. Physiol.* **284**, E177-E183.

Harris, K. P. and Tepass, U. (2008). Cdc42 and Par proteins stabilize dynamic adherens junctions in the Drosophila neuroectoderm through regulation of apical endocytosis. *J. Cell Biol.* **183**, 1129-1143.

Herrera, P. L. (2000). Adult insulin- and glucagon-producing cells differentiate from two independent cell lineages. *Development* **127**, 2317-2322.

Joberty, G., Petersen, C., Gao, L. and Macara, I. G. (2000). The cell-polarity protein Par6 links Par3 and atypical protein kinase C to Cdc42. *Nat. Cell Biol.* **2**, 531-539.

Kesavan, G., Sand, F. W., Greiner, T. U., Johansson, J. K., Kobberup, S., Wu, X., Brakebusch, C. and Semb, H. (2009). Cdc42-mediated tubulogenesis controls cell specification. *Cell* **139**, 791-801.

Kovacs, E. M., Verma, S., Ali, R. G., Ratheesh, A., Hamilton, N. A., Akhmanova, A. and Yap, A. S. (2011). N-WASP regulates the epithelial junctional actin cytoskeleton through a non-canonical post-nucleation pathway. *Nat. Cell Biol.* **13**, 934-943.

Lamarche, N., Tapon, N., Stowers, L., Burbelo, P. D., Aspenström, P., Bridges, T., Chant, J. and Hall, A. (1996). Rac and Cdc42 induce actin polymerization and G1 cell cycle progression independently of p65PAK and the JNK/SAPK MAP kinase cascade. *Cell* **87**, 519-529.

Lin, D., Edwards, A. S., Fawcett, J. P., Mbamalu, G., Scott, J. D. and Pawson, T. (2000). A mammalian PAR-3-PAR-6 complex implicated in Cdc42/Rac1 and aPKC signalling and cell polarity. *Nat. Cell Biol.* **2**, 540-552.

Lommel, S., Benesch, S., Rottner, K., Franz, T., Wehland, J. and Kühn, R. (2001). Actin pedestal formation by enteropathogenic Escherichia coli and intracellular motility of Shigella flexneri are abolished in N-WASP-defective cells. *EMBO Rep.* **2**, 850-857.

Marinari, E., Mehonic, A., Curran, S., Gale, J., Duke, T. and Baum, B. (2012). Live-cell delamination counterbalances epithelial growth to limit tissue overcrowding. *Nature* **484**, 542-545.

Matsuoka, T. A., Kaneto, H., Stein, R., Miyatsuka, T., Kawamori, D., Henderson, E., Kojima, I., Matsuhisa, M., Hori, M. and Yamasaki, Y. (2007). MafA regulates

expression of genes important to islet beta-cell function. *Mol. Endocrinol.* **21**, 2764-2774.
Metzger, D. E., Gasperowicz, M., Otto, F., Cross, J. C., Gradwohl, G. and Zaret, K. S. (2012). The transcriptional co-repressor Grg3/Tle3 promotes pancreatic endocrine progenitor delamination and β-cell differentiation. *Development* **139**, 1447-1456.
Pan, F. C. and Wright, C. (2011). Pancreas organogenesis: from bud to plexus to gland. *Dev. Dyn.* **240**, 530-565.
Percival, A. C. and Slack, J. M. (1999). Analysis of pancreatic development using a cell lineage label. *Exp. Cell Res.* **247**, 123-132.
Pictet, R. and Rutter, W. J. (1972). Development of the embryonic endocrine pancreas. In *Handbook of Physiology* (ed. D. Steiner and N. Freinkel), pp. 25-66. Washington, DC: American Physiological Society.
Pictet, R. L., Clark, W. R., Williams, R. H. and Rutter, W. J. (1972). An ultrastructural analysis of the developing embryonic pancreas. *Dev. Biol.* **29**, 436-467.
Rajput, C., Kini, V., Smith, M., Yazbeck, P., Chavez, A., Schmidt, T., Zhang, W., Knezevic, N., Komarova, Y. and Mehta, D. (2013). Neural Wiskott-Aldrich syndrome protein (N-WASP)-mediated p120-catenin interaction with Arp2-Actin complex stabilizes endothelial adherens junctions. *J. Biol. Chem.* **288**, 4241-4250.
Rohatgi, R., Ma, L., Miki, H., Lopez, M., Kirchhausen, T., Takenawa, T. and Kirschner, M. W. (1999). The interaction between N-WASP and the Arp2/3 complex links Cdc42-dependent signals to actin assembly. *Cell* **97**, 221-231.
Seymour, P. A. and Sander, M. (2011). Historical perspective: beginnings of the beta-cell: current perspectives in beta-cell development. *Diabetes* **60**, 364-376.
Soriano, P. (1999). Generalized lacZ expression with the ROSA26 Cre reporter strain. *Nat. Genet.* **21**, 70-71.
Theveneau, E. and Mayor, R. (2012). Neural crest delamination and migration: from epithelium-to-mesenchyme transition to collective cell migration. *Dev. Biol.* **366**, 34-54.
Villasenor, A., Chong, D. C., Henkemeyer, M. and Cleaver, O. (2010). Epithelial dynamics of pancreatic branching morphogenesis. *Development* **137**, 4295-4305.
Wodarz, A. and Huttner, W. B. (2003). Asymmetric cell division during neurogenesis in Drosophila and vertebrates. *Mech. Dev.* **120**, 1297-1309.

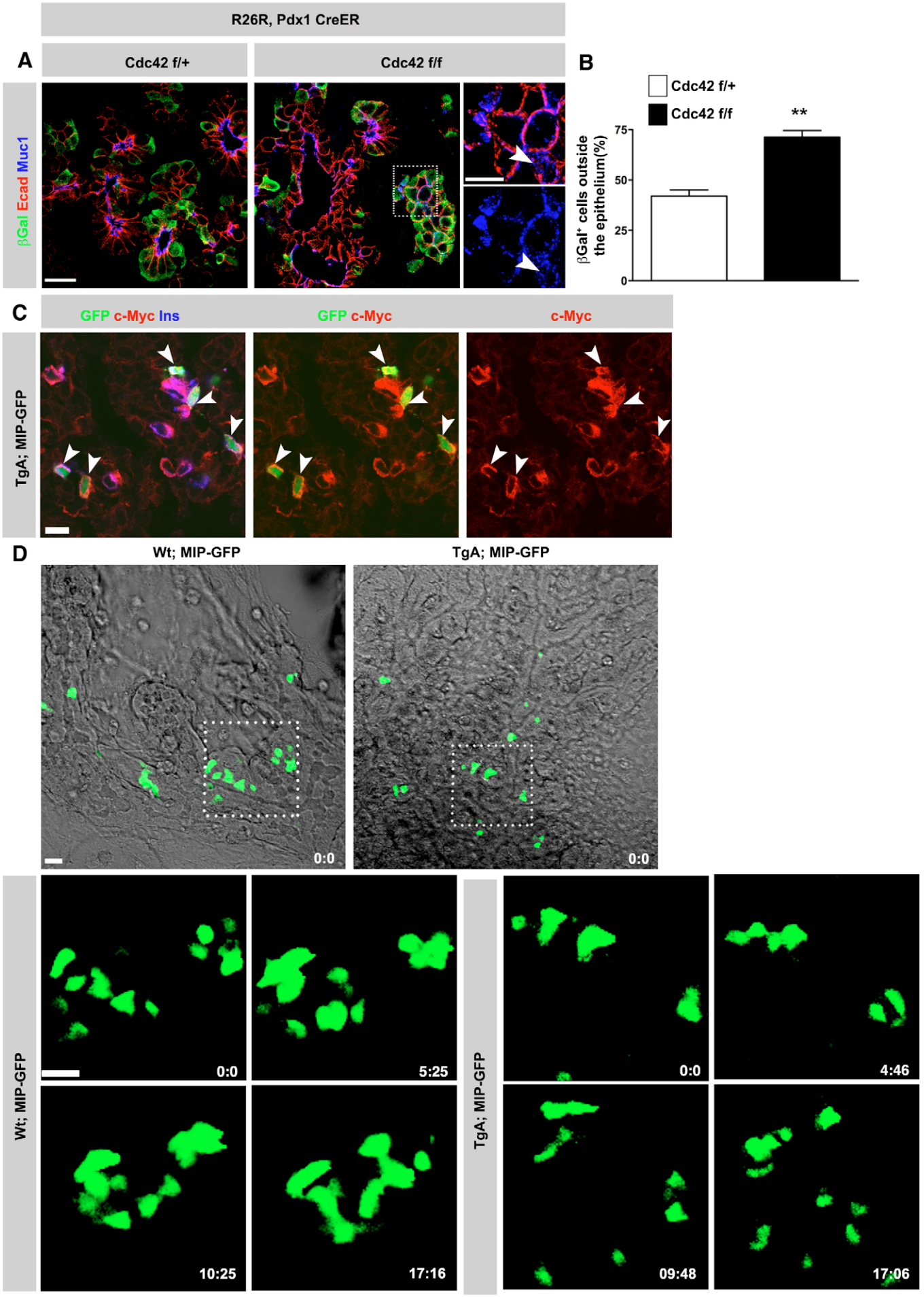
R26R, Pdx1 CreER
A
Cdc42 f/+
Cdc42 f/f
βGal Ecad Muc1
B
Cdc42 f/+
Cdc42 f/f
**
βGal+ cells outside the epithelium(%)
75
50
25
0
C
GFP c-Myc Ins
GFP c-Myc
c-Myc
TgA; MIP-GFP
D
Wt; MIP-GFP
TgA; MIP-GFP
0:0
0:0
Wt; MIP-GFP
0:0
5:25
10:25
17:16
TgA; MIP-GFP
0:0
4:46
09:48
17:06

Figure S1

Cdc42 ablation in polarised duct cells leads to delamination while expression of caCdc42

in beta cells impairs delamination

(**A**) Cdc42 heterozygote (*Cdc42 $^{f/+}$; Pdx1-cre^{ER}; R26*) and Cdc42 Knockout (*Cdc42 $^{f/f}$; Pdx1-cre^{ER}; R26R*) embryos were pulsed with tamoxifen at E12.5 and harvested at E15.5. At E15.5, about 16% of the epithelial cells have recombined, thereby creating a mosaic. Beta-galactosidase (βGal; green) marks the recombined cells. E-cadherin (Ecad; red) and mucin1 (Muc1; blue) mark the cell-cell contacts and apical surface of the epithelium, respectively. Images were acquired using a confocal microscope. In the Cdc42 heterozygote, βGal^{+} cells are located both within and outside the epithelium. In the Cdc42 knockout (KO), a significant number of KO cells delaminated and were located outside the epithelium. A selected region in the central panel (indicated with a box) is magnified on the adjacent right panel. The delaminated KO cells show intracellular Muc1 (arrowheads). The images are maximum intensity projections covering 10 μm.

(**B**) Graph showing the ratio of βGal^{+} cells that are outside the epithelium, relative to the total number of βGal^{+} cells. Compared to heterozygote (Cdc42 $^{f/+}$), more βGal^{+} cells were found outside the epithelium in the Cdc42 KO (Cdc42 $^{f/f}$), n= 3, p=0.0027.

Dorsal pancreas from Wt; MIP-GFP (GFP expression driven by the mouse insulin promoter) and TgA;MIP-GFP were harvested at E11.5 (day 0) and cultured in 2D on fibronectin-coated coverslips. The explants were imaged for 17 h from day 5 in a humidified chamber with CO_2. Both fluorescence and DIC images were sequentially captured every 15 minutes using z-stacks (35 to 50 μm) with an interval of 1-2 μm.

(**C**) Triple immunostaining of E15.5 MIP-GFP; caCdc42 (TgA) pancreas section with antibodies against GFP (green), c-Myc (red) and Ins (blue) showing co-expression of c-Myc and Insulin in all GFP^{+} cells (arrowheads). As the caCdc42 expression results in deficient beta cell differentiation (loss of insulin expression), a few c-Myc^{+} GFP^{-} cells were observed.

(**D**) Snapshot of Wt; MIP-GFP and Tg; MIP-GFP explants at the start of the movie (0 h), indicating the relative position of Ins^{+} cell clusters (green) to the epithelial and mesenchymal components. The white boxes indicate the regions which were analysed in detail during the time-lapse movies. The movement of Wt (left) and TgA (right) Ins^{+} cell clusters was tracked over time and representative snapshots at indicated time points (hours: minutes) are shown. The Ins^{+} cell clusters in the Wt aggregate and form larger clusters. In contrast, the Tg Ins^{+} cells show restricted cell movement, and fail to aggregate and generate large clusters.

Error bars represent SEM. Scale bar, 20 μm (A and D) and 10 μm (C).

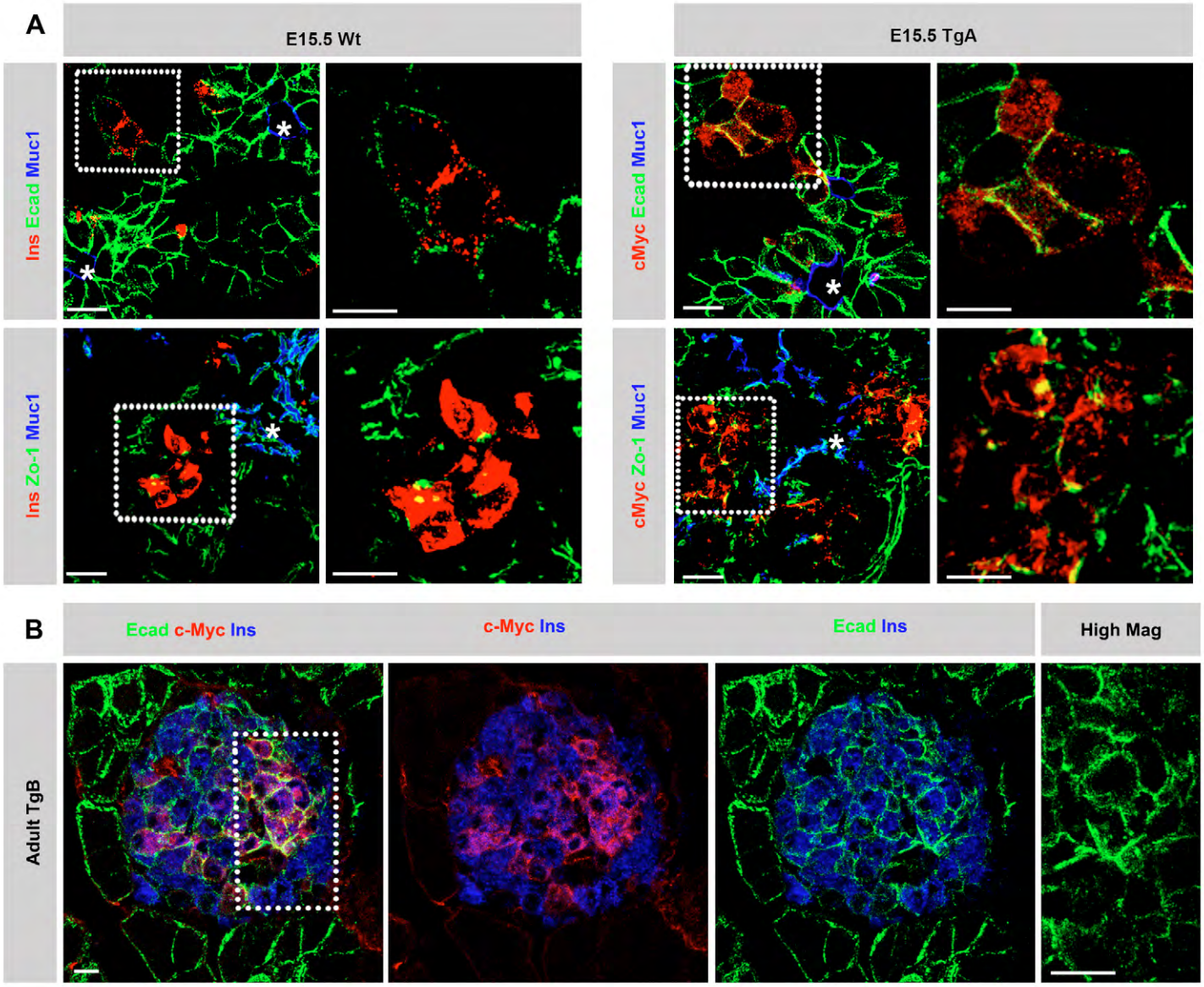

Figure S2

Impediment of cell-cell junction disassembly impairs beta cell delamination

(**A**) Sections of E15.5 pancreas from Wt and TgA were immunostained with antibodies against insulin (Ins; red) or c-Myc (red) in combination with Muc1 (blue), Ecad (green) and ZO-1 (green). The TgA Ins^{+} cells show similar expression levels of Ecad and ZO-1 compared to Wt beta cells. Images were acquired using a confocal microscope. Asterisks indicate lumens.

(**B**) Triple immunostainings of sections from 5-week old TgB pancreas with antibodies against Ecad (green)/c-Myc (red)/Ins (blue). Increased Ecad levels were observed at cell-cell contacts of TgB beta cells ($c\text{-}Myc^{+}Ins^{+}$) when compared to the Wt cells ($c\text{-}Myc^{-}Ins^{+}$). The regions indicated with a dotted square are magnified in the adjacent panel (High Mag).

The images are maximum intensity projections covering 10 µm sample height. Scale bar, 20 µm (A), 10 µm (B)

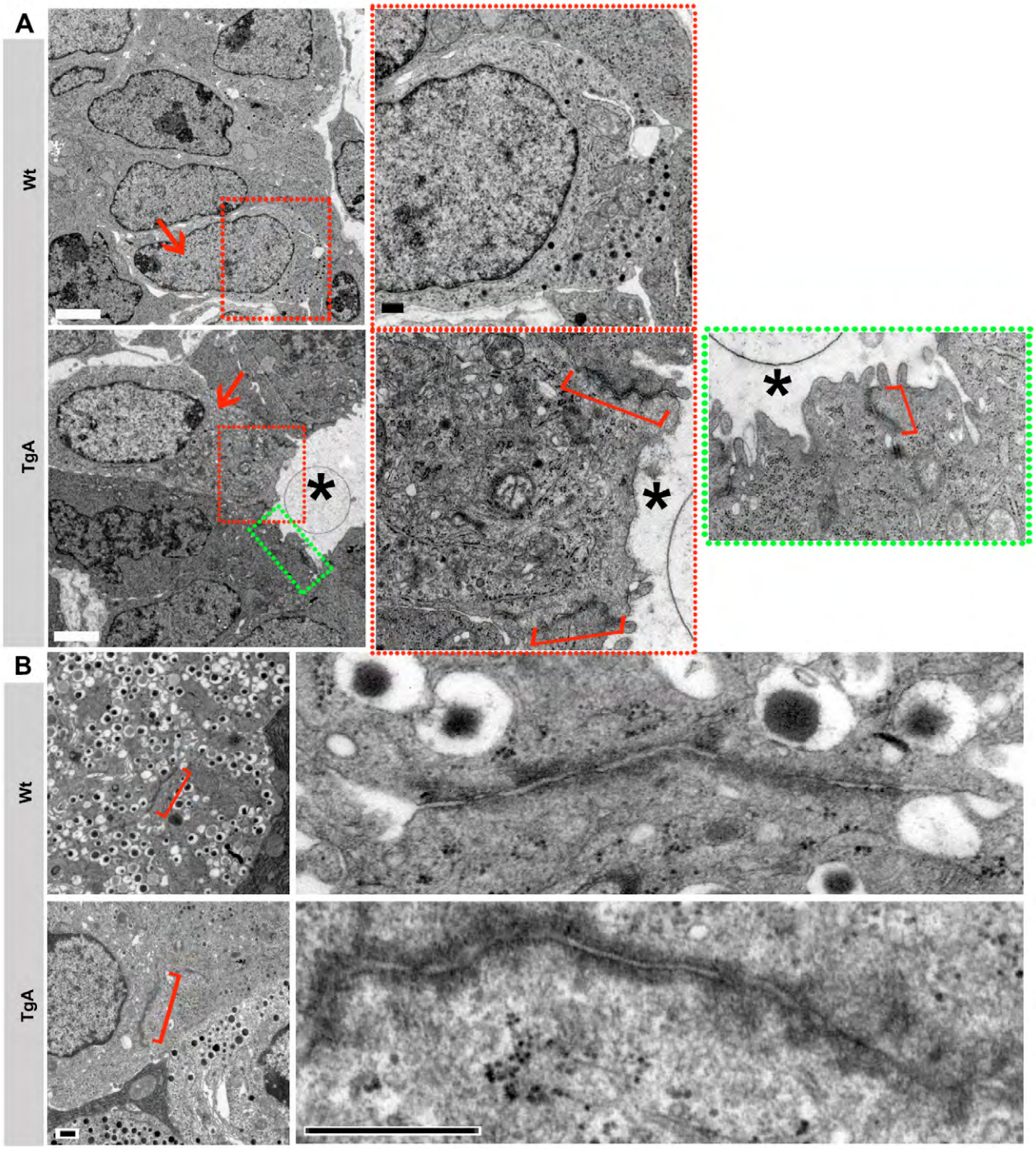

Figure S3

Enhanced junctional assembly of TgA beta cells

(**A**) Transmission electron microscopy (TEM) analysis of Wt and TgA pancreas at E15.5. Red arrows indicate Ins$^+$ cells. No junctional structures were evident in the Wt Ins$^+$ cells. In the TgA, junctions were found in between Ins$^+$ and the neighbouring "trunk cells" of the pancreatic epithelium. Note that only TgA Ins$^+$ cells could be observed facing the lumen. The dotted boxes marking the apical surface of the Ins$^+$ cell (red) and the neighbouring "trunk cells" of the pancreatic epithelium (green) are magnified in adjacent panels. The Ins$^+$ cell is flanked by the "trunk cells" on both sides and shows well-developed cell-cell junctions including abundant cortical F-actin bundles (red box). A representative image of the ultrastructural appearance of cell-cell junctions between "trunk cells" of the pancreatic epithelium (green box) is shown in the right panel. Brackets outline cell-cell junctions.

(**B**) TEM analysis of Wt and Tg islets from pancreas of 5-week old mice shows a more pronounced localisation of actin bundles at the cell junction of Tg Ins$^+$ cells compared to cell junctions of Wt Ins$^+$ cells. In addition, Tg cell junctions are longer compared to Wt. The cell junctions are marked with square brackets and magnified in the adjacent panel.

Scale bars, 1 μm (A) and 0.5 μm (B).

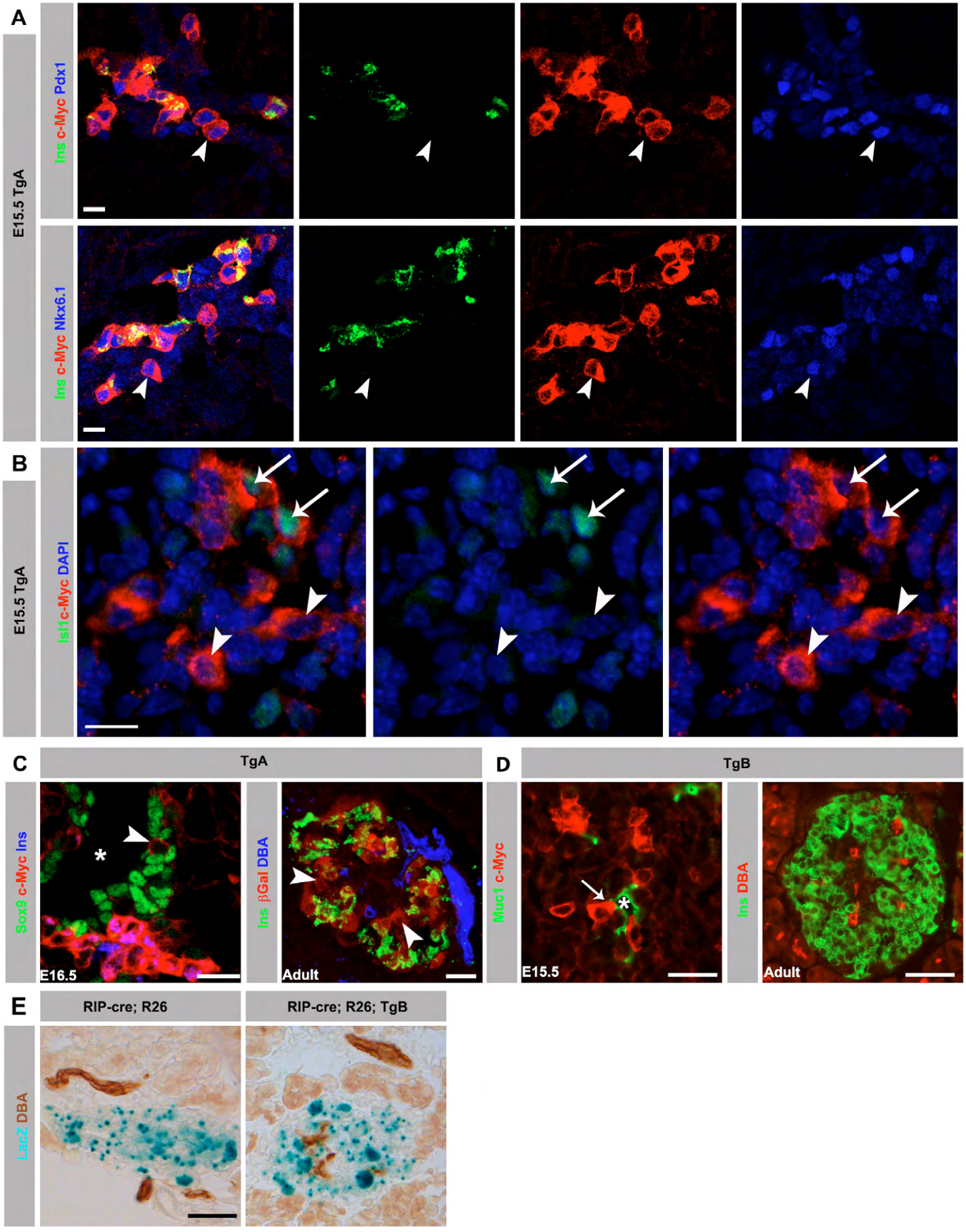
A
E15.5 TgA
Ins c-Myc Pdx1
Ins c-Myc Nkx6.1
B
E15.5 TgA
Isl1 c-Myc DAPI
C
TgA
Sox9 c-Myc Ins
E16.5
Ins βGal DBA
Adult
D
TgB
Muc1 c-Myc
E15.5
Ins DBA
Adult
E
RIP-cre; R26
RIP-cre; R26; TgB
LacZ DBA

Figure S4

Expression of caCdc42 impairs beta cell differentiation/maturation without affecting trans-differentiation

(**A**) Triple immunostainings using Insulin (green), c-Myc (red) and Pdx1 (blue, top panel) or Nkx6.1 (blue, lower panel). Both, Pdx1 and Nkx6.1 were present in c-Myc^{+}Ins^{-} cells (arrowheads).

(**B**) Triple immunostaining of sections from E15.5 TgA pancreas with antibodies against Isl1 (green) and c-Myc (red). Isl1 was absent in several c-Myc^{+}Ins^{-} cells (arrowheads), whereas maintained in others (arrows).

(**C**) Triple immunostaining of E16.5 TgA pancreas section with antibodies against c-Myc (red), primitive duct marker Sox9 (green) and Ins (blue). The c-Myc^{+}Ins^{-} transgenic cell facing the lumen (arrowheads) does not express Sox9, while the neighbouring trunk cells are Sox9^{+}, suggesting that TgA cell do not trans-differentiate into duct cells. Pancreas sections of 8-week old *TgA;RIP-cre;R26 LccZ* mice were triple immunostained with antibodies against beta-galactosidase (βGal; red), to irreversibly label Ins^{+} cells in combination with the duct marker DBA (blue) and Ins (green). The βGal staining was restricted to the islets. Notably, few Ins^{-}βGal^{+} cells were also observed within the islets (arrowheads), indicating that these cells expressed Ins at an earlier time point. In contrast, all DBA^{+} duct cells in the islets were βgal^{-}.

(**D**) Double immunostainings of E15.5 and adult TgB pancreas sections with antibodies against c-Myc (red) and Muc1 (green) (E15.5; left) and Ins (green) and DBA (red) (adult; right). At E15.5, the c-Myc^{+} cells remain within the epithelium and retain contact with the apical surface marked by Muc-1 (arrows). In the adult pancreas, intermingling of ducts within the islets was observed. Both the embryonic and adult phenotypes are identical to the TgA line.

(**E**) Lineage tracing analysis of the transgenic line TgB was carried out. Sections of adult TgB pancreas were stained for LacZ activity (blue) to trace the Ins^{+} cells and immunostained with the duct marker DBA (brown). In both Wt and TgB islets, the LacZ staining was restricted to beta cells, suggesting that TgB beta cells do not trans-differentiate into duct cells.

The images are maximum intensity projections covering 10 μm sample height. (A-D). Asterisks indicate lumens. Scale bars 20μm.

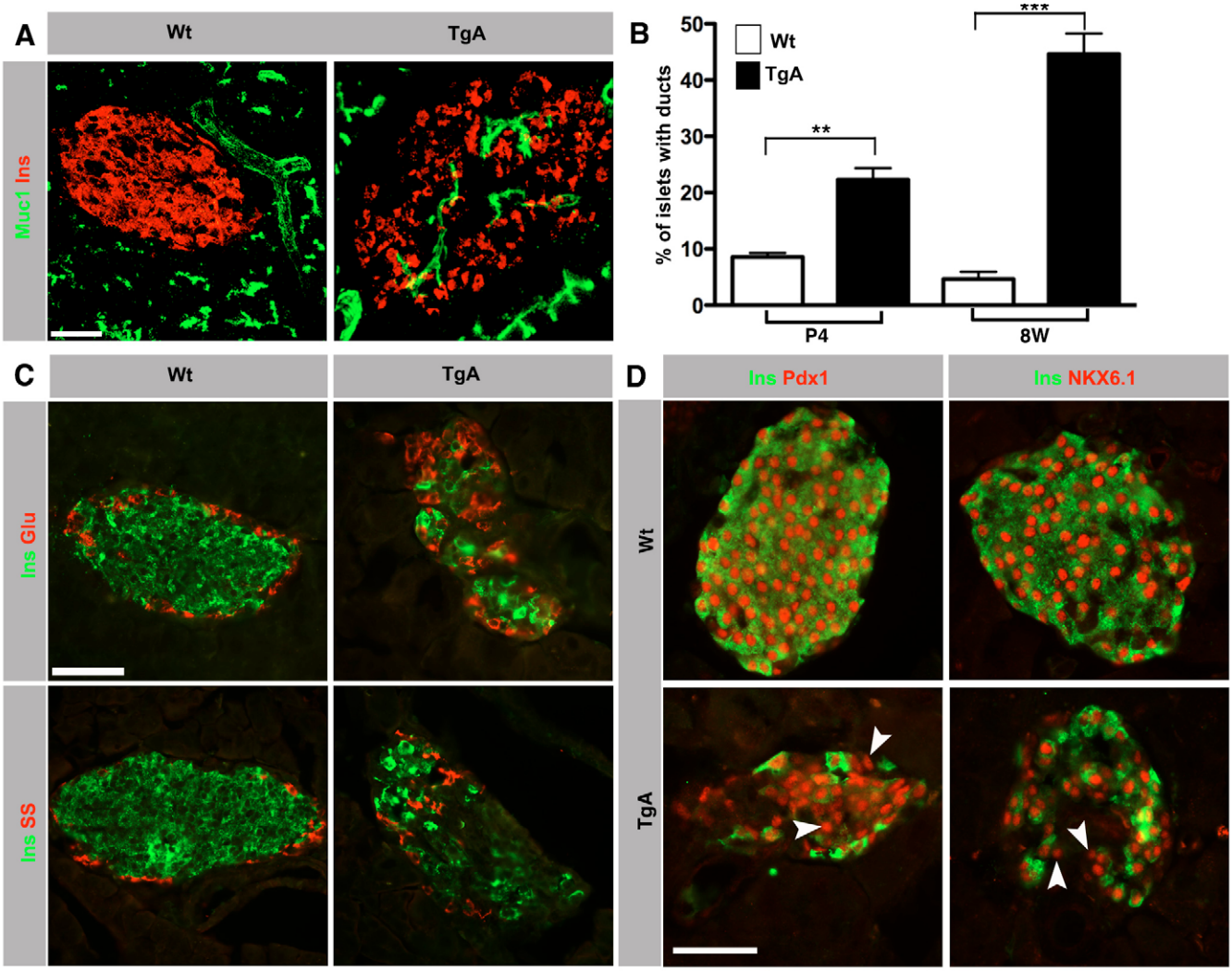
A
Wt
TgA
Muc1 Ins
B
Wt
TgA
% of islets with ducts
50
40
30
20
10
0
**
***
P4
8W
C
Wt
TgA
Ins Glu
Ins SS
D
Ins Pdx1
Ins NKX6.1
Wt
TgA

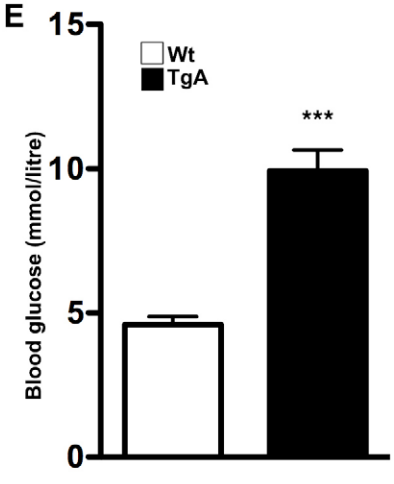
E
Wt
TgA
Blood glucose (mmol/litre)
15
10
5
0
***

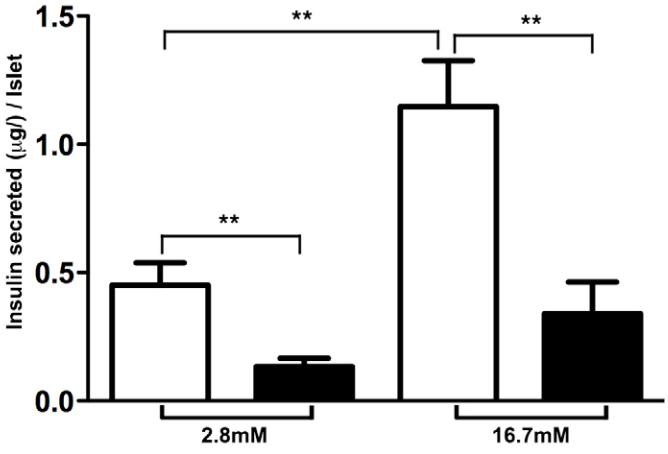
F
Insulin secreted (µg/) / Islet
1.5
1.0
0.5
0.0
**
**
**
2.8mM
16.7mM

Figure S5

Expression of caCdc42 in beta cells results in aberrant islet morphogenesis and impaired glucose homeostasis

(**A**) Double immunostainings of sections from adult Wt and TgA pancreas (5 weeks) with antibodies against Muc1 (green) and Ins (red). Wt Ins^+ cells cluster into circular islets, which segregate from ducts, whereas TgA Ins^+ cells cluster into more irregularly shaped islets wherein islet cells are intermingled with ducts. These are maximum intensity projection images covering 30 μm sample height.

(**B**) Quantifications showing the percentage of islets with ducts at P4, Wt 8.5% vs. TgA 22%, p=0.0031; 8 weeks, Wt 4.6% vs. TgA 44.6%, p=0.0005. n=3.

(**C**) Double immunostainings of sections from adult Wt and TgA pancreas (5 weeks) with antibodies against somatostatin (SS, red) or glucagon (Glu, red) and Ins (green). In Wt islets, Glu^+ and SS^+ cells are distributed along the periphery of the islet, whereas TgA islets show a scattered distribution of Glu^+ and SS^+ cells.

(**D**) Double immunostainings of sections from adult Wt and TgA pancreas (5 weeks) with antibodies against Pdx1 (red) or Nkx6.1 (red) and Ins (green). Both Pdx1 and Nkx6.1 are expressed at Wt levels in the majority of TgA Ins^+ cells. In fact, even Ins^- TgA cells maintain Pdx1 and Nkx6.1 expression (arrowheads).

(**E**) Higher fasting blood glucose was observed in TgA animals (5 weeks) compared to their Wt littermates. n=5, p=0.0005.

(**F**) Glucose-stimulated insulin secretion assays were carried out on islets isolated from Wt (4 animals) and TgA (5 animals). Wt islets increase insulin secretion in response to glucose while TgA islets secrete less insulin in the unstimulated state compared to Wt islets and fail to increase insulin secretion upon glucose stimulation. n represents number of wells analysed (3 islets /well). 2.8mM, Wt (n=21) versus TgA (n=14), p=0.0071; 16.7mM, Wt (n=21) versus TgA (n=16), p=0.0014; Wt, 2.8mM versus 16.7mM, p=0.0012; TgA, 2.8mM versus 16.7mM, p=0.1378.

Images were acquired using confocal microscopy. Scale bar 20 μm (A, C and D).

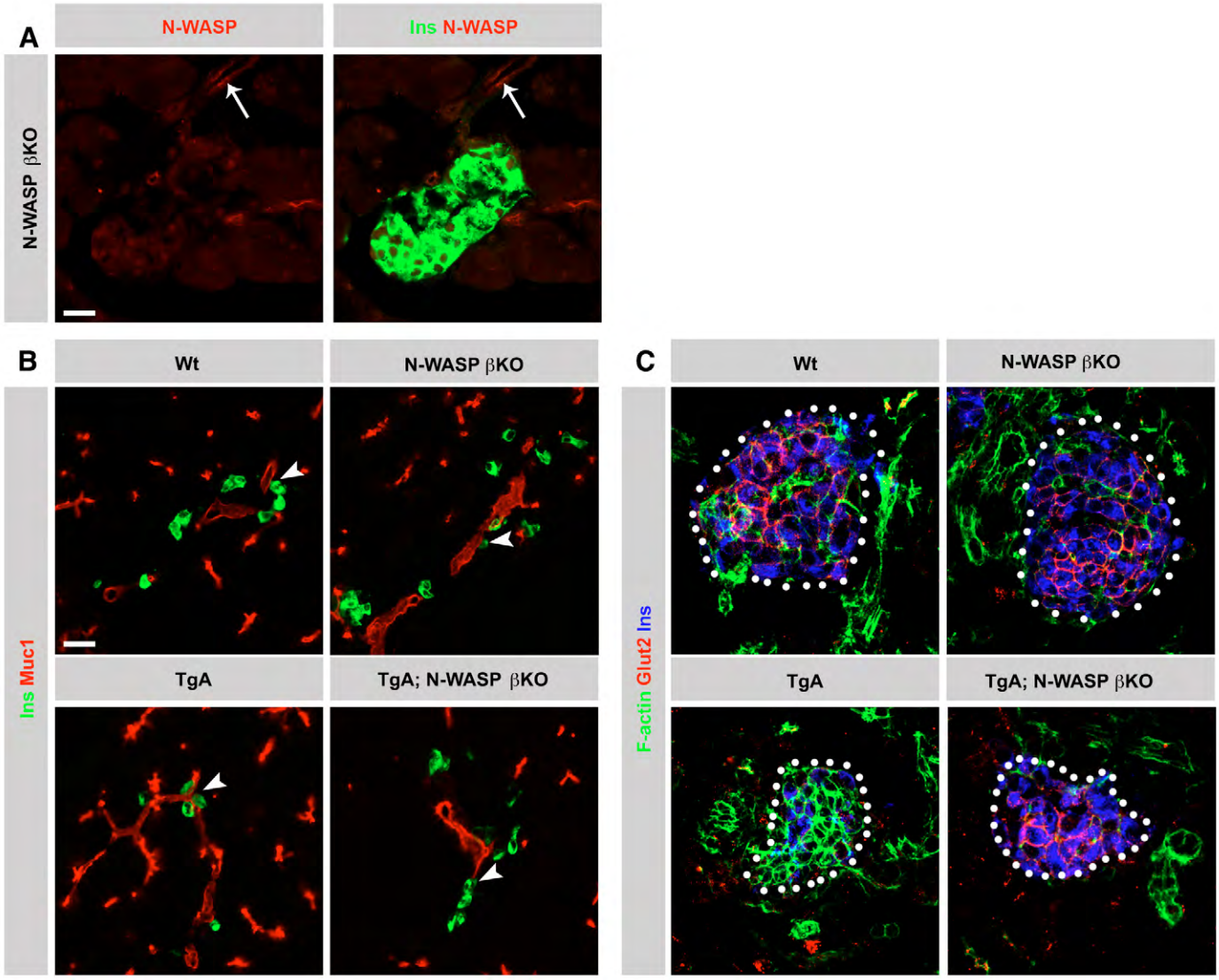

Figure S6

Ablation of N-WASP partially restores caCdc42- induced inhibition of beta cell delamination

(**A**) Double immunostaining of P4 sections from Wt and TgA pancreas with antibodies against N-WASP (red) and Insulin (Ins, green). The N-WASP βKO shows loss of N-WASP protein expression in beta cells, while N-WASP expression in the ducts (arrows) remains unaffected. Section thickness, 10 μm.

(**B**) Double immunostainings of sections from P4 Wt, N-WASP βKO, TgA and TgA;N-WASP βKO pancreata with antibodies against Ins (green) and Muc1 (red) showing distribution of Ins^+ cells in contact with $Muc1^+$ lumens (indicated with arrowheads). The lower panel highlights the partial rescue of beta cell delamination in the TgA;N-WASP βKO mice (for quantification, see Figure 8C). Section thickness, 10 μm.

(**C**) Sections of P4 Wt, N-WASP βKO, TgA and TgA;N-WASP βKO pancreata were immunostained with antibodies against F-actin (green), Glut2 (red) and Ins (blue). Islets were identified using Ins staining and are marked with dotted circles (The individual channels are shown in Figure 8A).

Scale bars 20 μm (A and B)

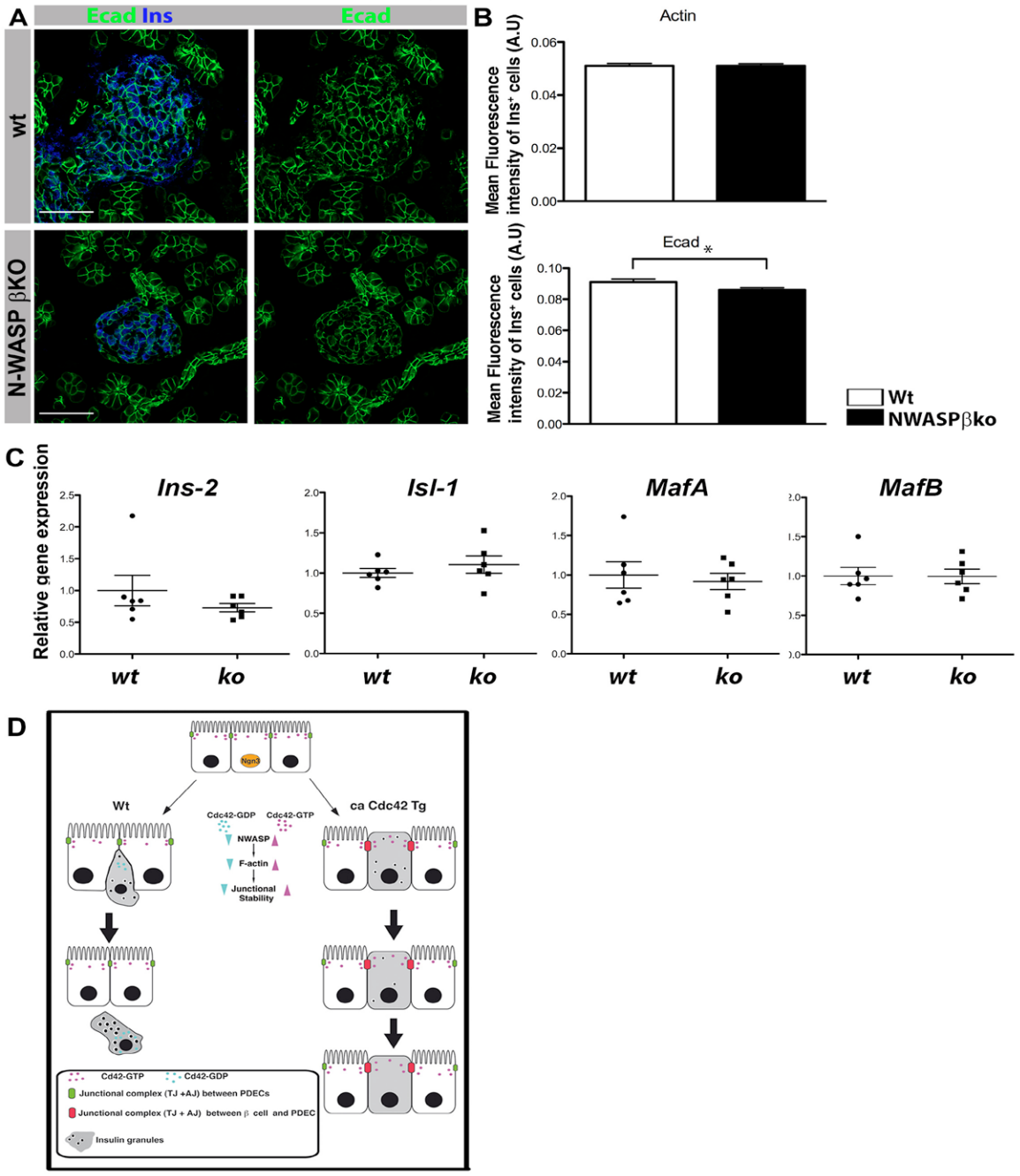

Figure S7 Reduced E-cadherin in N-WASPβKO beta cells

(**A**) Double immunonstainings of sections from P4 Wt (upper row) and N-WASPβKO (lower row) using antibodies against Ecad (green) and Insulin (blue). Ecad expression appears to be reduced in N-WASPβKO beta cells. Section thickness, 10 µm.

(**B**) Quantification of the mean fluorescence intensity of F-actin and Ecad immunostainings in P4 Ins^+ cells revealed a slight reduction in Ecad intensity in N-WASPβKO Ins^+ cells compared to Wt Ins^+ cells. The expression of F-actin remained unchanged. At least three embryos for each genotype were analyzed. n represents number of Ins^+ cells; n= 654 (Wt) and 676 (N-WASPβKO), p> 0.05 (F-actin) and p=0.02 (Ecad).

(**C**) Q-PCR analysis of P4 Wt and N-WASPβKO pancreata show a normal relative expression of *Ins2* (p=0.30), *Isl1* (p=0.40) and *MafA* (p=0.68) and *MafB* (p=0.97) in N-WASPβKO in comparison to Wt. (Wt, n=6 and N-WASPβKO n=6).

(**D**) Schematic illustration of the proposed model for beta cell delamination. Active Cdc42 (Cdc42-GTP) via N-WASP prevents the delamination of $Ngn3^+$ endocrine precursors from the epithelium by maintaining apical polarity and stable cortical F-actin and cell-cell junctions. Delamination of newly born beta cells requires the inactivation of Cdc42 (Cdc42-GDP), which in turn results in the loss of apical polarity, and disassembly of the cortical F-actin network and cell-cell junctions.

Scale bar 50µm. Error bars represent SEM.

Movie 1

Time lapse imaging of Ins^+ cells in Wt; MIP-GFP shows beta cell delamination, migration and clustering. The Ins^+ cell (indicated with arrows) delaminates and migrates towards an extra-epithelial Ins^+ cell cluster. The day of the harvest (E11.5) was marked day 0. Starting from day 5, the explants were imaged for about 17 hours.

Movie 2

Time lapse imaging of TgA; MIP-GFP shows markedly restricted movement of the transgenic Ins^+ cell (top; centre) and subsequently these cells fail to delaminate. The day of the harvest (E11.5) was marked day 0. Starting from day 5, the explants were imaged for about 19hrs and 30 minutes.

Supplementary table 1. List of Antibodies used.

Antibody	Raised in	Dilution	Source
Beta Galactosidase	Rabbit	1:1000	ICN
c-Myc	Mouse	1:200	Evan et al 1985
Cdc42 (11A11)	Rabbit	1:500	Cell Signaling
DBA		1:1000	Vector
E-cadherin	Rat	1:200	Takara
Glucagon	Guinea pig	1:800	Linco
Glut2	Rabbit	1:100	Millipore
Insulin	Guinea pig	1:800	Dako
Islet1	Rabbit	1:100	Millipore
Ki67	Rabbit	1:100	Neomarkers
Laminin	Rabbit	1:500	Sigma
MafA	Rabbit	1:100	Bethyl Laboratories
Mucin 1	Armenian hamster	1:500	Neomarkers
N-WASP	Rabbit	1:100	S. Lommel

N-WASP (30D10)	Rabbit	1:500	Cell Signaling
Neurogenin3	Mouse	1:2000	BCBC
Nkx6.1	Rabbit	1:2000	BCBC
p-N-WASP	Rabbit	1:250	ECM Bioscience
Pdx1	Guinea pig	1:500	C.Wright
Pdx1	Goat	1:1000	C.Wright
Sox9	Rabbit	1:800	Chemicon
Somatostatin	Rabbit	1:500	Sigma
Vinculin	Mouse	1:1000	Sigma
ZO-1	Rabbit	1:100	Invitrogen

Supplementary Table 2. Q-PCR primers.

Gene	Primer Pair
Ins2	5'-CCC TGC TGG CCC TGC TCTT -3' 5'-AGG TCT GAA GGT CAC CTG CT-3'
HPRT	5'-AGCCCCAAAATGGTTAAGGT-3' 5'-CAAGGGCATATCCAACAACA-3'
Isl1	5'-CGGAGAGACATGATGGTGGTT-3' 5'-GGCTGATCTATGTCGCTTTGC-3'
MafA	5'-CCTGTAGAGGAAGCCGAGGAA-3' 5'-CCTCCCCCAGTCGAGTATAGC-3'
MafB	5'-GGCAACTAACGCTGCAACTCT-3' 5'-CAACGGAAGGGACTTGAACAC-3'

Reference for supplementary data

Evan GI, Lewis GK, Ramsay G. & Bishop JM. (1985). Isolation of monoclonal antibodies specific for human c-myc proto-oncogene product. *Mol Cell Biol* **5**: 3610-3616.